

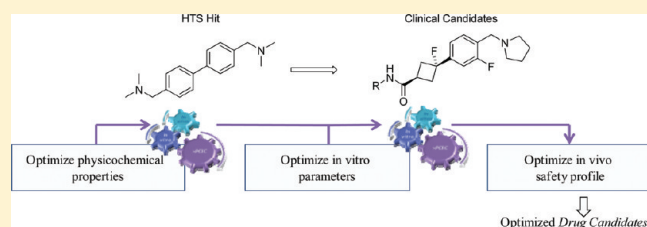
Discovery of Two Clinical Histamine H₃ Receptor Antagonists: *trans*-*N*-Ethyl-3-fluoro-3-[3-fluoro-4-(pyrrolidinylmethyl)-phenyl]cyclobutanecarboxamide (PF-03654746) and *trans*-3-Fluoro-3-[3-fluoro-4-(pyrrolidin-1-ylmethyl)phenyl]-*N*-(2-methylpropyl)cyclobutanecarboxamide (PF-03654764)

Travis T. Wager,^{*,†} Betty A. Pettersen,[†] Anne W. Schmidt,[†] Douglas K. Spracklin, Scot Mente, Todd W. Butler, Harry Howard, Jr, Daniel J. Lettiere, David M. Rubitski, Diane F. Wong, Frank M. Nedza, Frederick R. Nelson, Hans Rollema, Jeffrey W. Raggon, Jiri Aubrecht, Jody K. Freeman, John M. Marcek, Julie Cianfroga, Karen W. Cook, Larry C. James, Linda A. Chatman, Philip A. Iredale, Michael J. Banker, Michael L. Homiski, Jennifer B. Munzner, and Rama Y. Chandrasekaran

Groton Laboratories, Pfizer Worldwide Research and Development, 558 Eastern Point Road, Groton, Connecticut 06340-5159, United States

S Supporting Information

ABSTRACT: The discovery of two histamine H₃ antagonist clinical candidates is disclosed. The pathway to identification of the two clinical candidates, **6** (PF-03654746) and **7** (PF-03654764) required five hypothesis driven design cycles. The key to success in identifying these clinical candidates was the development of a compound design strategy that leveraged medicinal chemistry knowledge and traditional assays in conjunction with computational and in vitro safety tools. Overall, clinical compounds **6** and **7** exceeded conservative safety margins and possessed optimal pharmacological and pharmacokinetic profiles, thus achieving our initial goal of identifying compounds with fully aligned oral drug attributes, “best-in-class” molecules.



■ INTRODUCTION

Histamine receptors have been attractive and druggable targets for decades.^{1,2} Histamine H₁ receptor antagonists, such as diphenhydramine and those that have limited central nervous system (CNS) exposure such as cetirizine and fexofenadine, are successful allergy medications. Histamine H₂ receptor antagonists such as ranitidine and famotidine have proved to be efficacious gastric ulcer treatments. While the histamine H₃ and H₄ receptors are also considered attractive and druggable targets, no marketed agents currently exist for these receptors. Preclinical activity is high, and early clinical candidates have been disclosed targeting histamine H₃ receptors.^{3,4} Herein we describe the discovery of selective histamine H₃ receptor antagonists.

Histamine has high affinity for H₃ receptors. The highest density of H₃ receptors is in the brain, primarily in prefrontal regions, where histamine seems to play a key role in a variety of centrally mediated functions including attention and learning/memory, as well as arousal and wakefulness.^{5,6} Histamine levels oscillate over a 24 h period, with concentrations highest during the day and lowest at night. Furthermore, CNS-penetrant H₁ receptor antagonists induce marked sedation⁷ and impairment of cognitive performance, suggesting that histamine (HA) is involved in maintaining wakefulness and may promote enhanced attention and/or vigilance during the waking state. Some histamine H₃ receptors are inhibitory autoreceptors that regulate the

synthesis and release of histamine (Figure 1A).⁸ Other H₃ receptors are heteroreceptors that regulate the release of neurotransmitters including dopamine (DA) and norepinephrine (NE), such that an H₃ receptor antagonist should increase levels of these other neurotransmitters in the synapse (Figure 1B).^{6,9} However, not all H₃ receptor antagonists have the same effects on neurotransmitter release; for example, some H₃ antagonists increase DA and NE levels while others do not.¹⁰ In addition, H₃ receptors can regulate the release of acetylcholine (ACh), a neurotransmitter involved in cognition.⁹

Collectively, the knowledge around histamine and H₃ receptors suggests that antagonism of the H₃ receptor is a potential therapeutic target for treatment of attention deficit hyperactivity disorder (ADHD), narcolepsy, Alzheimer's disease (AD), and possibly other cognitive disorders. The cardinal symptoms of ADHD include impulsive behavior, hyperactivity, and inattention. Typically, the hyperactivity component seen in school-age children does not continue into adulthood, whereas the attention and impulsivity symptoms do persist. The psychostimulant methylphenidate, as well as other agents that successfully treat ADHD symptoms, elevates extracellular levels of dopamine and norepinephrine in the CNS. Recent microdialysis studies in rats show

Received: July 14, 2011

Published: September 19, 2011

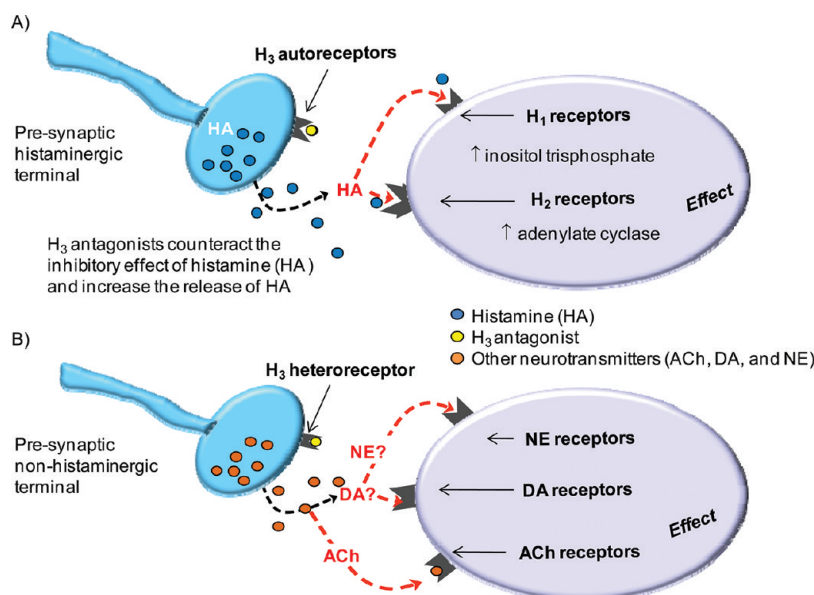


Figure 1. (A) Histaminergic neuron. H_3 autoreceptor, endogenous histamine (HA), acts at presynaptic H_3 autoreceptors to reduce HA synthesis and release (a negative feedback loop). (B) Nonhistaminergic neuron. Blockade of the H_3 heteroreceptors should modulate the release of other neurotransmitters.

that methylphenidate also increases levels of histamine and acetylcholine.^{11,12} Although psychostimulants are highly effective agents for treatment of patients with ADHD, there are several drawbacks: these agents produce decreased appetite, insomnia, upset stomach, and headache and additionally have abuse potential, leading to their classification as scheduled drugs. Atomoxetine, a norepinephrine reuptake inhibitor that is also approved to treat ADHD, acts by increasing extracellular levels of NE and DA, as well as HA and ACh, in prefrontal areas of the brain.^{11,12} Although atomoxetine is not a scheduled agent, some safety liabilities have been reported and it bears a black box warning regarding liver toxicity.^{13,14} Clearly, an unmet medical need exists in this area.

Herein we describe the discovery of selective histamine H_3 receptor antagonists to treat CNS disorders. Our goal was to identify H_3 receptor antagonists that elevate HA and ACh levels in rat prefrontal cortex in vivo, possess a predicted pharmacokinetic (PK) profile consistent with q.d. or b.i.d. dosing in humans, and demonstrate a safety profile beyond standard margins in preclinical safety studies, as we were interested in considering a pediatric indication for ADHD. The work described here focuses less on in vitro potency, structure–activity relationships (SARs), and in vivo potency (typical medicinal chemistry benchmarks) and more on development of the strategy we used to identify safe and druglike molecules at the design stage, early in the drug discovery process.

RESULTS AND DISCUSSION

Initial HTS Screen and Analysis of Hits. The original H_3 hit **1** (Figure 2) was identified from a high-throughput binding screen and exhibited high affinity for human H_3 receptors ($K_i = 1.3$ nM). Structurally related hits (data not shown) were selective versus other biogenic amine receptors and had weak hERG inhibition as measured using a whole-cell voltage clamp technique ($IC_{50} > 5600$ nM).¹⁵ By use of a high-throughput in vitro human liver microsome (HLM) assay and an in silico model of estimated microsomal free fraction ($cf_{u,mic}$), the unbound microsomal

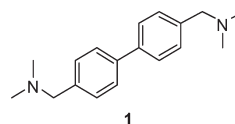


Figure 2. H_3 receptor antagonist **1** emerged from a high-throughput screen (HTS). Subsequent to our identification of HTS hit **1**, it was reported in the literature by Morini et al.²³

intrinsic clearance ($CL_{int,u}$) for **1** was determined to be unacceptably high ($CL_{int,u} = 219$ mL min⁻¹ kg⁻¹).^{16,17} In addition to this rapid clearance, two other significant issues with **1** needed to be addressed. First, the compound had been reported as a curarizing (muscle-relaxant) agent,¹⁸ and second, the planar nature of the biphenyl motif could pose genetic safety issues. We were concerned with the potential long-term safety risks inherent in a linear rigid chemotype that could ultimately result in costly late-stage safety attrition (phase 3 or postmarketing).

Exposure to polycyclic aromatic hydrocarbon compounds has been shown to increase genotoxic risk,¹⁹ and a crystal structure of nogalamycin in DNA revealed that bulky dumbbell-shaped molecules can intercalate between DNA base pairs.²⁰ Further, dicationic amidine compounds have been reported to bind in the DNA minor groove.²¹ Thus, our primary concern was that the biaryldiamine template could act as a DNA-binding agent scaffold, producing genetic damage and increasing patients' cancer risk. The initial in vitro micronucleus (IVMN) screening result was negative for **1**, but we remained apprehensive about idiosyncratic toxicity for this general chemotype. Further supporting our safety concerns, Hancock et al. reported positive findings in an IVMN assay for several biaryl H_3 receptor antagonists.²² To reduce the potential liability of the biaryl template, we searched for an aryl isostere that could mimic the distance between the two basic groups. We hypothesized that a cyclobutyl moiety might act as such an aryl ring isostere (Figure 3A). Molecular modeling supported this hypothesis: minimized structures of biaryl and

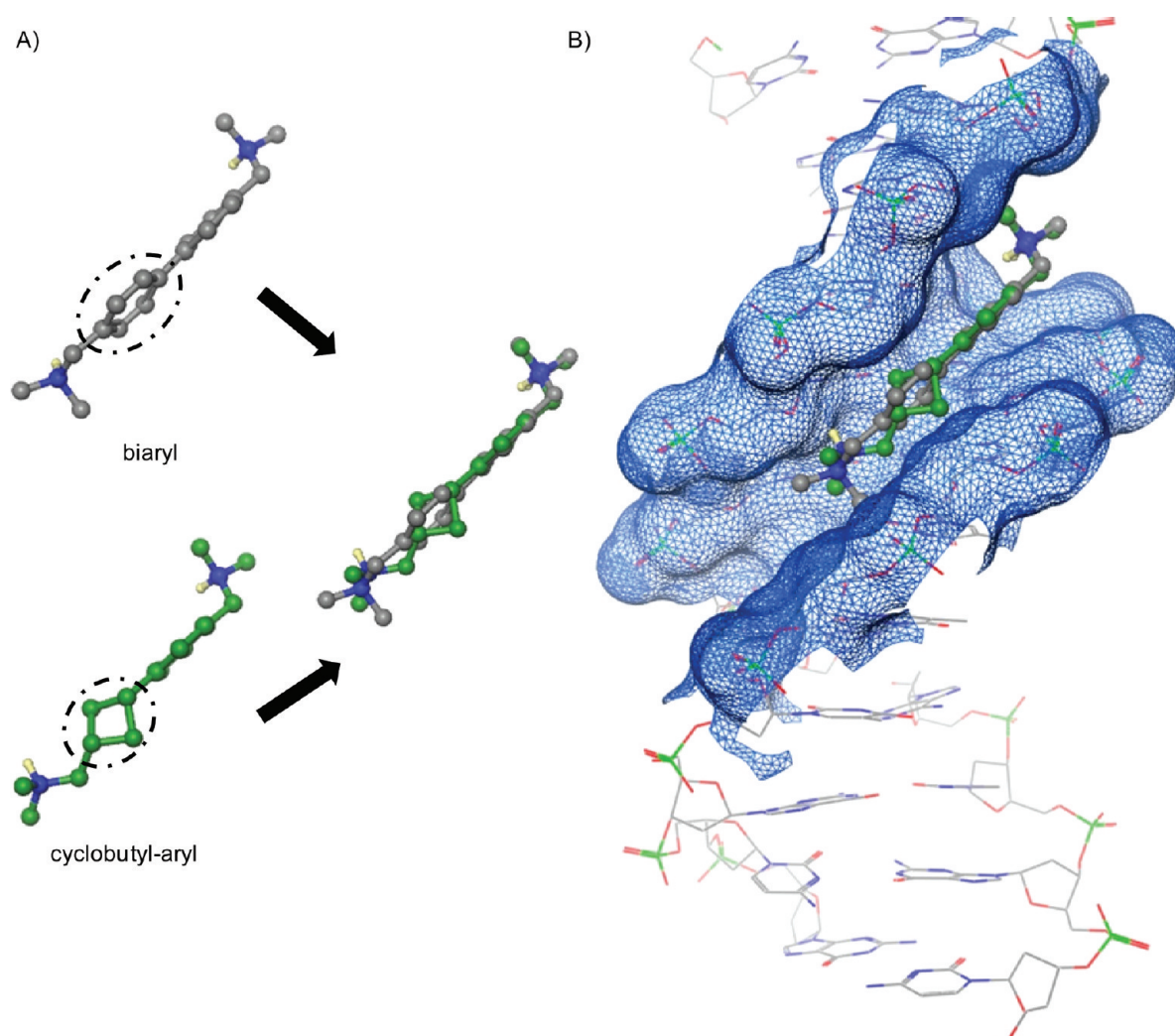


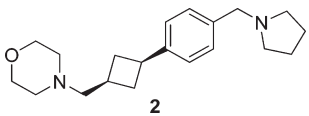
Figure 3. (A) Isostere analysis of biaryl moiety vs cyclobutylaryl, where the black oval denotes motifs to be compared (isostere): molecular modeling and overlap of biaryl (gray) and cyclobutylaryl (green) compounds. The two nitrogen atoms maintain an approximately equal distance from each other in both molecules. (B) Same molecular overlap matched to surface of DNA structure (in blue, PDB code 302D). As designed, the cyclobutyl ring (green) is not a matched fit in the minor groove of DNA because of the bulkier cyclobutyl ring relative to the biaryl motif (gray).

arylcyclobutyl cores exhibited good overlap of the basic groups (Figure 3A).

In addition, we hypothesized that because of the three-dimensional shape (3D-volume) of the cyclobutyl-containing moiety, this moiety would be less likely to bind in the minor groove. Using the X-ray crystal structure of a known minor groove-binding drug (HOECHST 33258) bound to DNA as a template,²⁴ we examined the overlay matched to the surface volume of DNA (Figure 3B). While the biaryl motif matches well, the cyclobutyl rotates in a manner that gives a far worse fit. Although the quality of fit was not quantified, we felt the synthetic chemistry investment was worth the risk to test these hypotheses. If one aryl group could be replaced with a cyclobutyl isostere, we could potentially accomplish two goals: (1) building a novel core and (2) increasing our odds of avoiding genetic toxicity.

Design of the Initial Lead Compound (2). To test whether replacing the biaryl moiety of the HTS hit **1** could be accomplished, an extensive set of dibasic cyclobutyl analogues was synthesized (see section Chemistry for synthesis). This synthetic effort yielded numerous compounds that maintained the potency

attribute of the HTS hit **1**. Of the 286 dibasic cyclobutyl analogues synthesized, one compound (**2**) possessed the profile we sought for a potential drug candidate (Table 1). Compound **2** had a high affinity for both the human and rat H₃ receptors (K_i of 2.2 and 7.7 nM, respectively) and demonstrated antagonist activity in adenylate cyclase assays in both human and rat cell lines expressing H₃, with K_i of 0.89 and 3.5 nM, respectively. To assess selectivity, **2** was screened in a broad pharmacological panel, both in-house and externally (CEREP), and exhibited greater than 100-fold selectivity versus other biogenic amine receptors, enzymes, and transporters (see Supporting Information). In addition, **2** had a good early safety profile, as characterized by a lack of projected drug–drug interactions (DDI),²⁵ extremely weak hERG inhibition (hERG IC_{50} = 300 μ M),¹⁵ and negative results in the Bioluminescence Assay (IVMN), and human lymphocyte (HLA) assays.²⁷ Finally, the pharmacokinetic profile of **2** was excellent, with low HLM clearance in vitro ($CL_{int,u}$),¹⁶ high MDCK (Madin–Darby canine kidney) passive apparent permeability,²⁸ and a low P-gp efflux ratio (ER) (see Table 1).²⁸ Thus, our goal of replacing one aryl ring with a cyclobutyl moiety while maintaining affinity for

Table 1. Selected Physicochemical Properties, in Vitro Characteristics, and Safety and ADME Data for **2**


parameter ^a	value
ClogP	3.6
ClogD _{7.4}	−0.2
MW	314
TPSA	15.7
pK _a	9.8 and 7.7
H ₃ K _i functional antagonist (human) ^b (nM)	0.89
hERG IC ₅₀ ^c (μM)	300
IVMN ^d	negative
CL _{int,u} ^e (mL min ^{−1} kg ^{−1})	<10
MDCK AB ^f (cm/s)	>10 × 10 ^{−6}
P-gp ER ^g	<1
rat f _{u,p}	0.72

^a Calculated physicochemical properties were obtained using standard commercial packages: Biobyte for ClogP calculations, ACD/Labs for ClogD at pH 7.4 and the most basic pK_a. ^b Human functional assay measuring cAMP utilizing a reporter gene assay (β-lactamase) in HEK293 cells stably expressing human H₃ receptor. K_i is the geometric mean of five independent experiments. ^c Blockade of the hERG potassium channel in HEK293 cells.^{15 d} In vitro micronucleus assay. ^e Human liver microsome unbound intrinsic clearance. ^f MS-based quantification of apical → basolateral transfer rate of a test compound at 2 μM across contiguous monolayers of MDCK cells. ^g Ratio of (basal → apical) to (apical → basal) transfer rate of a test compound at 2 μM across contiguous monolayers of MDR1-transfected MDCK cells.

the H₃ receptor and minimizing the potential genetic toxicity was realized through the discovery of **2**.

The central nervous system effect of **2** was demonstrated using the *R*-α-methylhistamine (RAMH) induced dipsogenia model.^{29,30} Compound **2** dose-dependently blocked RAMH-induced water drinking in rats with a subcutaneous ID₅₀ of 0.78 mg/kg (*N* = 1 experiment). The free drug levels were calculated using plasma protein binding (f_{u,p}) measurements from a separate in vitro assay and determined to be 23.0 nM, approximately 3-fold higher than the K_i (rat H₃ binding K_i = 7.7 nM). This result (3-fold the rat H₃ binding K_i) is consistent with antagonist pharmacology requiring >75% receptor occupancy for efficacy.³¹ To allow comparisons between the safety profiles of lead compounds, this benchmark (3-fold K_i) is used throughout this manuscript as the projected clinically efficacious concentration (PCEC). One assumption made in this comparison was that all compounds freely cross the blood–brain barrier such that the ratio unbound brain (C_{b,u})/unbound plasma (C_{p,u}) is equal to 1.

Phospholipidosis. Compound **2** met or exceeded our initial in vitro and in vivo efficacy criteria and was advanced into a 4-day oral dose study in rats (3/sex per dose) to assess safety. Several doses were tested in that study (5, 50, and 400 mg/kg). At 5 mg/kg (mean AUC of 1245 ± 659 ng·h/mL) there were no findings. At ≥50 mg/kg, phospholipidosis (kidney and lung) was seen (mean AUC of 17375 ± 6983 ng·h/mL), while mortality was observed at 400 mg/kg (mean C_{max} of 3918 ± 1280 ng/mL). Phospholipidosis was confirmed in the lung and kidney by electron

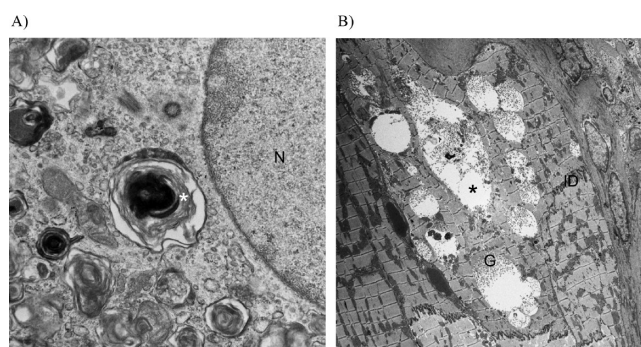


Figure 4. (A) Electron microscopy image of rat lung, phospholipidosis “foamy macrophage” induced by **2** in drug-treated group at 400 mg/kg: multilamellated bodies (*); *N* = nucleus; TEM 10000× magnification. (B) Electron microscopy image of drug storage. Cytoarchitecture of dog heart includes the presence of multiple cardiomyocyte vacuoles (CMV, *) induced by **2** within the cytoplasm of cardiomyocytes: ID = intercalated disk of cardiac muscle; G = glycogen; TEM 1000× magnification.

microscopic examination, which revealed multilamellated membranous lysosomal inclusions commonly referred to as multilamellar bodies or MLBs (Figure 4A). These whorls are the hallmark of phospholipidosis (PL), a storage disorder resulting in excessive accumulation of phospholipids in lysosomes of the tissues. The risk associated with compound-induced PL was considered manageable provided that an acceptable therapeutic index (TI) existed and that the effect was reversible.³² On the basis of these findings, we embarked on an in vivo derisking strategy requiring longer exploratory toxicology studies (14 days in rat) that included an arm for reversibility of the PL finding (14-day washout period), as well as a toxicology study in a second species (dog). The next step with **2** was to conduct a 14-day study in rats (7 males/dose) to determine if the threshold for phospholipidosis decreased with increased duration of treatment (14 days versus 4 days). This 14-day study (5–30 mg/kg) indicated that the threshold for phospholipidosis did not decrease with longer treatment. In fact, no PL was observed at the highest tested dose (30 mg/kg) tested. The safety margin for phospholipidosis was large in rat, ≥588-fold PCEC (Table 11, Materials and Methods). Although the safety profile from these rat studies was favorable, a concurrent 7-day study in dogs (3 dogs at 10 and 25 mg/kg) identified a new finding at all tested doses: cardiomyocyte vacuoles (CMV) were observed in heart tissue at low multiples of the PCEC (<17-fold, Table 11). The CMV were specifically located in the cardiac papillary muscle and characterized as drug storage vacuoles (Figure 4B). This safety finding (CMV) was not manageable, as it had a low TI and no biomarker to guide clinical safety. The CMV safety findings observed in dogs precluded **2** from moving into regulatory toxicity studies.

In summary, while the initial design objective was achieved, two unexpected findings arose for the dibasic chemotype, both centered on safety (PL and CMV). Given the fact that our most advanced chemical matter attrited in later-stage safety studies, the discovery effort cycled back to the compound design stage and our initial strategy was re-evaluated. We asked ourselves the following question: “Was de-risking PL the ideal approach?” Our conclusion was “no”, that a better strategy, if possible, would be to design molecules that did not induce PL. We therefore set a conservative safety standard for compound progression: a compound would not advance if it caused PL in vivo at otherwise tolerated doses. It was hypothesized that moving to a more

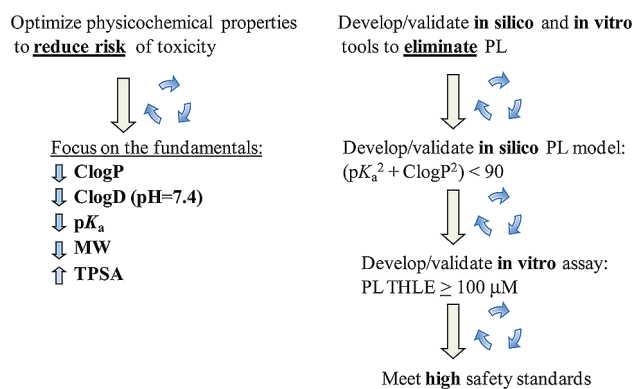


Figure 5. Development of a design strategy to remove safety liabilities. The two-pronged strategy uses prospective design (focusing on optimal physical properties) and the development and validation of an in vitro screening assay to identify PL liability at an early stage.

favorable physicochemical property space could avoid this safety finding.^{33,34} To increase our odds of success, in addition to physicochemical property optimization, we also needed to develop a way to rank compounds according to their PL risk. Ideally, one would be able to evaluate PL at the design stage and then re-evaluate after synthesis. Rather than focusing on a single property, in silico model, or in vitro end point, we employed a multipronged design strategy (Figure 5). As part of this approach, we needed to prospectively incorporate medicinal chemistry knowledge around central nervous system (CNS) drugs into our design.^{34–40} First, at the design stage we worked toward optimizing physicochemical properties by lowering (a) lipophilicity, as assessed by calculated partition coefficient (ClogP), (b) distribution coefficient at pH 7.4 (ClogD), (c) molecular weight (MW), and (d) calculated pK_a of the most basic center. Simultaneously, we focused on developing and validating both an in silico PL model and an in vitro PL assay. Although we generated an in-house statistical PL model (not discussed herein), we chose to use the intuitive PL model described by Ploemen.⁴¹ Ploemen et al. reported that if the sum of the squares of the pK_a and ClogP values for a compound is greater than or equal to 90, then the compound is at higher risk of causing PL in vivo. Given the fact that H_3 is a biogenic amine receptor and our current hits possessed a basic amine, it was clear that lowering the pK_a was potentially the most direct way to bring the calculated value into a more desirable range. Indeed, the pK_a contribution value in Ploemen's PL model accounted for the largest part of the sum of the squares ($pK_a = 9.8$, $9.8^2 = 96$). A second factor we considered was that a dibasic compound may doubly impact the PL finding, which is not accounted for in Ploemen's PL model. Thus, in addition to the in silico PL model, we examined an in vitro PL cell-based assay to serve as a surrogate for in vivo study and thus improve our odds of identifying a safe molecule. Generation of the in vitro PL values was accomplished using a method similar to that recently reported by Morelli et al.⁴² For the work describe herein, phospholipid accumulation was assessed in a transformed human liver epithelial (THLE) cell line and reported as a minimum effect dose (MED) value in μM , where lower MED values (see Materials and Methods for details) predict a greater risk of PL in vivo.

In addition, we needed to understand the cause of CMV or, at a minimum, develop a strategy that would remove this safety liability. Parallel SAR efforts (data not discussed herein) allowed us to conclude that the CMV safety finding was not a direct result

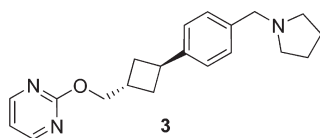
Table 2. Safety Studies of Two Literature Compounds: Disobutamide and Bidisomide^{43,44}

Compound	Structure	Preclinical safety study findings	Basic pK_a
disobutamide		clear cytoplasmic vacuoles in various tissues of dogs and rats	10.5, 9.5
bidisomide		no clear cytoplasmic vacuoles observed	9.5

of antagonizing the H_3 receptor, as the evaluation of alternative chemotypes did not show this toxicity. Hjelle et al. reported that disobutamide was a potent inducer of clear cytoplasmic vacuoles in various tissues (Table 2).⁴³ The authors described disobutamide as a molecule that possessed a dibasic motif and they associated this structural feature with the observed toxicity. The clear cytoplasmic vacuoles described by Hjelle et al. seemed similar to those we observed, except that we observed them only in the cardiac papillary muscle. Their solution to the clear cytoplasmic vacuole problem was to remove or mask one of the basic amines (Table 2). All this information suggested to us that elimination of the CMV safety finding might be accomplished by simply removing one basic center. It was crucial, of course, to demonstrate that potency, safety attributes, and the desired absorption, distribution, metabolism, and excretion (ADME) profiles could be retained in a monobasic molecule.

Optimized Lead Compound 3. The overall compound design objective seemed simple enough: find a safe and well-tolerated H_3 receptor antagonist that would test the H_3 hypotheses in the clinic. For the next design cycle we employed the new design strategy highlighted above (Figure 5). The physicochemical properties of **2** that we considered optimal were its low MW (314 Da), moderate ClogP, low ClogD, and moderate to high basicity (pK_a of basic centers of 7.2 and 9.8). At the time of our initial work we tracked topological polar surface area (TPSA)⁴⁵ and ClogP as a surrogate for volume of distribution (tissue distribution), which is thought to be a major factor contributing to in vivo PL.⁴⁶ On the basis of a recent analysis by Hughes et al., this combination may have even more general utility as an early in vivo safety odds predictor.³³ Topological polar surface area for **2** was undesirable (15 \AA^2) based on the cutoff ($>75 \text{ \AA}^2$) provided by Hughes et al.³³ These authors concluded that compounds possessed a greater safety risk when dual conditions $\text{ClogP} > 3$ and $\text{TPSA} < 75 \text{ \AA}^2$ were satisfied (odds of seeing an adverse event at a total plasma level of $10 \mu M$ test compound).³³ We used **2** as a baseline for comparison and to benchmark progress for all later compounds. (Baseline values for **2** were the following: PL in silico value of 109 (19 higher than the target value 90) and in vitro PL MED = $37.5 \mu M$, target value of $\geq 100 \mu M$.) Employing this new design strategy, we set out to identify a compound with improved attributes.

The next compound that we identified with a suitable profile was **3** (Table 3). Monobasic compound **3** met all of our pharmacology and ADME criteria (Tables 7–10) and most of our early safety targets. The physicochemical properties of **3** were similar to those of **2**, with the most notable improvement being

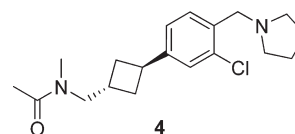
Table 3. Monobasic Cyclobutylaryl H₃ Receptor Antagonist 3

parameter ^a	value
ClogP	4.0
ClogD _{7.4}	0.8
MW	323
TPSA	38
pK _a	9.8
Early PL Safety Assessment	
in silico PL	112
PL MED ^b (μM)	119.5

^a Calculated physicochemical properties were obtained using standard commercial packages: Biobyte for ClogP calculations, ACD/Labs for ClogD at pH 7.4 and the most basic pK_a. ^b Transformed human liver epithelial cellular phospholipidosis assay measuring phospholipid accumulation per cell. Compounds were classified as positive at the lowest dose for which the induction of phospholipid accumulation was 3-fold over background. MED value is the geometric mean of three independent experiments.

removal of one of the basic amines. The in silico PL value increased to a less desirable value (112), driven by higher lipophilicity relative to 2 (ClogP of 3.6 → 4.0), but the in vitro PL value shifted upward toward a more favorable value (MED = 119 μM), meeting our target in this regard. Compound 3 was synthesized on scale (see Chemistry) and tested in a 14-day rat safety study (3/sex per dose). Given the potential risk of seeing PL in vivo, we elected to run three doses in this safety study (5, 50, 350 mg/kg). Phospholipidosis was observed in multiple tissues (lung and liver) at ≥ 50 mg/kg (mean AUC 21,333 ± 7,146 ng·h/mL, day 1). As stated earlier, our compound selection criteria precluded compounds that exhibited PL in vivo, so this compound's development was terminated (TI ≥ 7 PCEC; see Table 11). The in silico PL model value (112 versus target 90) suggested an enhanced risk of PL in vivo, and this prediction was consistent with the 14-day safety study findings wherein PL was observed. We therefore placed more weight on this design parameter in subsequent work. On the other hand, the in vitro PL assay results had suggested a reduced risk of in vivo PL for 3 versus 2, which was not observed. At this time we did not abandon the PL assay because we believed that there would still be benefit in rank-ordering compounds via an in vitro assay. Having established that a monobasic compound could provide a candidate profile, the next generation compound was also designed to be monobasic.⁴³ Further, the use of both the in silico PL model and the in vitro PL assay was retained within the design strategy to better guide compound selection, and we anticipated allowing some flexibility in application of the PL models based on holistic assessment of scores. We felt that using hard cutoff values would restrict design space and perhaps cause undue hardship in the identification of a potent and safe H₃ receptor antagonist.

Next Generation Lead Compound (4). Earlier work from our laboratories (not described herein) suggested that substantially lowering the pK_a of the remaining basic amine (pK_a decreased

Table 4. Monobasic H₃ Receptor Antagonist, 4 with Reduced pK_a Relative to Parent Compound 2

parameter ^a	value
ClogP	3.3
ClogD _{7.4}	0.8
MW	335
TPSA	24
pK _a	9.3
Early PL Safety Assessment	
in silico PL	98
PL MED ^b (μM)	245.3

^a Calculated physicochemical properties were obtained using standard commercial packages: Biobyte for ClogP calculations, ACD/Labs for ClogD at pH 7.4 and the most basic pK_a. ^b Transformed human liver epithelial cellular phospholipidosis assay measuring phospholipid accumulation per cell. Compounds were classified as positive at the lowest dose for which the induction of phospholipid accumulation was 3-fold over background. MED value is the geometric mean of three independent experiments.

from 9.8 to 7.6) resulted in a significant drop in affinity for the H₃ receptor. We therefore set out to identify a compound with only a moderate reduction in basicity (pK_a decreased to ~9) that retained a high affinity for the H₃ receptor. From this effort, 4 was identified (see Chemistry for synthesis) as the next generation H₃ receptor antagonist (Table 4). Compound 4 met our pharmacology and ADME criteria (Tables 7–10) but now with an improved in silico PL value (98) and in vitro PL assay value (MED = 245 μM) relative to 2 and 3. Although compound 4 did not meet the in silico PL target value of ≤ 90, the markedly increased in vitro PL value was encouraging. The physicochemical properties of 4 were desirable, with low MW, reduced ClogP, increased TPSA, and a reduction in the pK_a of the most basic center (Figure 6). The half log unit reduction in pK_a (from 9.8 to 9.3) relative to the parent compound (2) was achieved through incorporation of a halogen atom at the 2-position of the phenyl ring. Compound 4 was evaluated in a 14-day toxicology study in rats (6 males/dose) over a dose range of 10 to 300 mg/kg. All doses were well tolerated, and most importantly no PL was observed (mean AUC of ≤ 4444 ng·h/mL, day 1) (≥ 36 PCEC, Table 11). These findings suggested that the improved design strategy (monobasic, moderate reduction of pK_a) was a viable approach for the identification of a PL-free compound and that the in vitro PL assay provided significant value. Notably, had we driven decisions using a sharp cutoff in the in silico PL value, we would not have made this compound (PL = 98). The successful completion of the 14-day toxicology study in rats justified further investment in compound 4. A second species toxicology study, 7-day study in dogs (2/sex), was initiated at 50 mg/kg (mean AUC of 4777 ± 1970 ng·h/mL, day 1). This dose was lowered to 30 mg/kg on day 2 because of convulsions in 2 of 4 dogs following a single dose at 50 mg/kg (C_{max} of 3200–6200 ng/mL). The dose was maintained at 30 mg/kg for the rest of this study (mean AUC of 2911 ± 626 ng·h/mL, day 7). Given the fact that

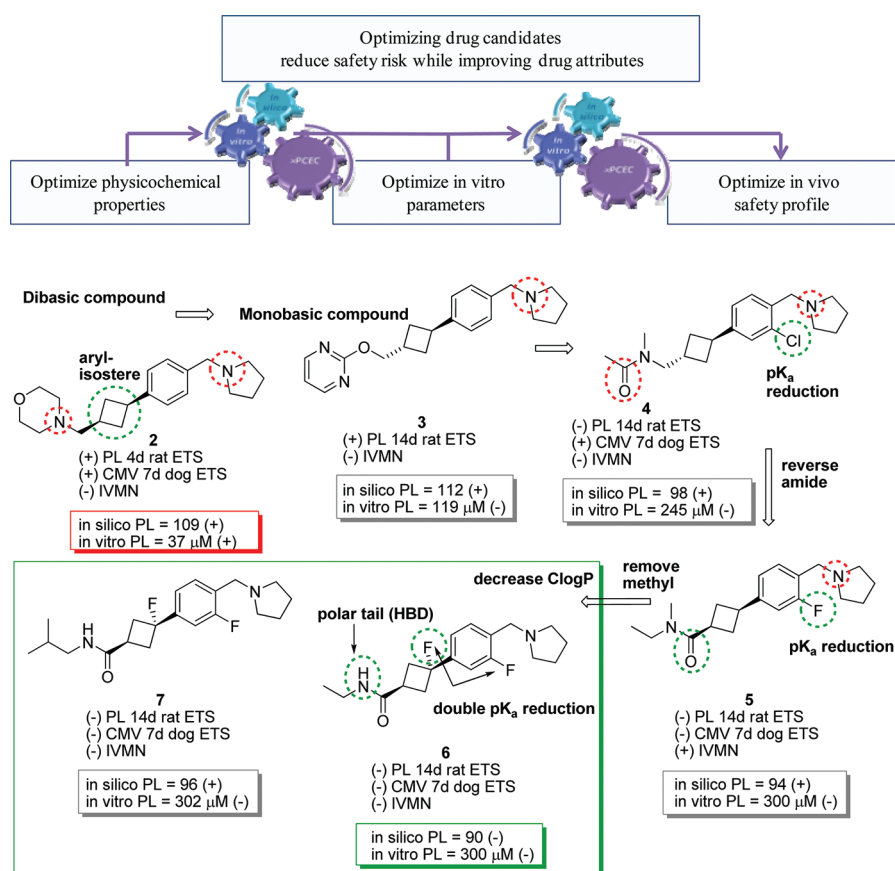
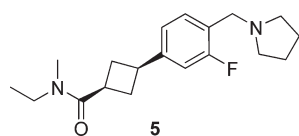


Figure 6. Path to the H₃ receptor antagonist clinical candidates. The red circles represent areas targeted for improvement, and the green circles represent improvements made to that molecule. The in silico phospholipidosis (PL) cutoff of ≤ 90 and the in vitro PL assay target of $\geq 100 \mu\text{M}$ were used to identify compounds with reduced risk of observing PL in vivo. Labels + (finding) and – (no findings) denote risk in in vitro micronucleus (IVMN) or findings for phospholipidosis (PL) and cardiomyocyte vacuoles (CMV) in an exploratory toxicology study (ETS).

4 was well-tolerated in the 14-day study in rats, we did not anticipate any problems in the 7-day study in dogs. However, testicular degeneration and CMV were observed at low multiples of the projected clinically efficacious concentration (<29 PCEC, Table 11). The findings in the papillary region of the heart were similar to the CMV observed in dogs with 2 and precluded further development of this compound. On the basis of previous exploratory toxicology studies of monobasic compounds (data not shown), it was not clear why CMV were observed with this monobasic chemotype. One possible explanation was that hydrolysis of the amide yielded a dibasic metabolite that produced CMV in the 7-day dog safety study. While we had no direct evidence that metabolism of the amide in compound 4 yielded the free amine, the clinical use of *N*-acyl prodrugs of amines makes this a reasonable hypothesis.⁴⁷ In any case, the identification of a compound without an in vivo PL safety liability was a major advancement. We attributed this success to a design strategy that leveraged our understanding of how physicochemical properties affect in vivo safety and appropriate utilization of in silico PL model values and in vitro PL assay data.

Addressing CMV. Lead Compound 5. The hypothesis that in vivo amide cleavage of 4 occurred and that the resulting metabolite was responsible for the CMV finding seemed plausible. In the next generation molecule, we therefore sought a compound that possessed all the desired attributes achieved with 4 but lacked the potential to generate a dibasic metabolite. This design

strategy resulted in discovery of the potent H₃ receptor antagonist 5 (Table 5). Structurally, 5 differs from 4 in two key features: first, the *exo*-amide is internalized, and second, the chlorine atom has been replaced by a fluorine. Metabolic cleavage of the *endo*-amide would provide a carboxylate moiety, avoiding the potential issues with a dibasic metabolite. We hypothesized that such a carboxylate metabolite would not cause CMV. The fluorine atom served the same purpose as the original chlorine atom (reduction of pK_a) but with the added benefit of reducing MW (335 \rightarrow 318) and lipophilicity (ClogP = 3.3 \rightarrow 2.6). Compound 5's pharmacology, ADME (Tables 7–10) and early safety attributes were similar to those of 4; in addition, it displayed a comparable in silico PL value (94) and in vitro PL assay value (MED = 300 μM). A 14-day toxicology study in rats (6 males/dose) was conducted with 5 over a dose range of 10–300 mg/kg, and no PL was observed (AUC up to 35600 ng·h/mL). Further, this compound was well tolerated up to a high multiple of the projected clinically efficacious concentration (≥ 371 PCEC, Table 11). These data supported further development. A single-dose study in dogs (1/sex per dose at 10 and 50 mg/kg; 1 male dog/dose at 75 and 100 mg/kg) identified 50 mg/kg (C_{max} of 5875 ± 2227 ng/mL) as the maximum tolerated dose for a subsequent 7-day study. In this 7-day study in dogs (2/sex), the dose was lowered from 50 mg/kg (mean C_{max} of 12859 ± 4473 ng/mL, day 1) to 25 mg/kg on day 2 because of convulsions in 2 of 4 dogs at 50 mg/kg. The dose was maintained at 25 mg/kg (mean AUC of 10780 ± 1368 ng·h/mL,

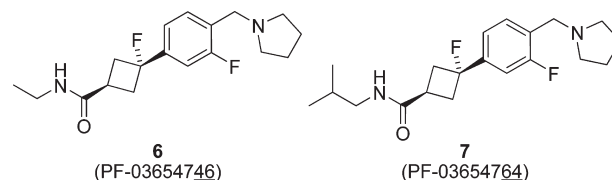
Table 5. Monobasic H₃ Receptor Antagonist 5 with *endo*-Amide Replacing the *exo*-Amide of Compound 4

parameter ^a	value
ClogP	2.6
ClogD _{7.4}	0.4
MW	318
TPSA	24
pK _a	9.3
Early PL Safety Assessment	
in silico PL	94
PL MED ^a (μM)	300.0

^a Calculated physicochemical properties were obtained using standard commercial packages: Biobyte for ClogP calculations, ACD/Labs for ClogD at pH 7.4 and the most basic pK_a. ^a Transformed human liver epithelial cellular phospholipidosis assay measuring phospholipid accumulation per cell. Compounds were classified as positive at the lowest dose for which the induction of phospholipid accumulation was 3-fold over background. MED value is the geometric mean of three independent experiments.

day 7 values) for the remainder of the study. Excellent drug exposure was achieved in this 7-day study, and there was no histological evidence of CMV (≥ 777 PCEC, Table 11). The next-generation lead compound **5** therefore met all of our criteria to move forward into clinical development. The redesigned H₃ receptor antagonist (*endo*-amide) yielded a compound that not only retained the potency attributes of **4** but also improved the overall safety profile (no CMV). The continual refinement of the physicochemical properties, in silico PL value, and in vitro PL value, coupled with further compound design (*exo*- to *endo*-amide), resulted in retention of druglike attributes (potency, specificity, ADME, and safety alignment), yielding a compound that moved forward in the drug development process. Unfortunately, genetic toxicology screening revealed a positive signal in the IVMN.²⁷ Follow-up testing indicated that the increased incidence of micronuclei resulted from an equal contribution of chromosome breakage and chromosome loss/gain. At this point we had the option to further characterize the risk of these findings and attempt to move **5** forward despite its genetic safety liability. In pursuit of a “best-in-class” molecule, however, we decided to further improve upon the profile of **5** and eliminate the genotoxic liability.

Final Drug Candidates 6 (PF-03654746) and 7 (PF-03654764).⁵² In the context of remaining true to our design strategy, we considered the possibility that an amplified electrostatic potential within the core of compound **5** might have a beneficial effect with respect to the IVMN liability. Our next design cycle focused on identifying where we could incorporate a fluorine atom without decreasing affinity for the H₃ receptor. We selected the cyclobutyl ring based on the assumption that the resulting compound would retain affinity for the H₃ receptor. The additional fluorine served two purposes: (1) to perturb any interactions with DNA that potentially existed with **5** and (2) to provide a long-range electron-withdrawing effect that should

Table 6. Clinical H₃ Histamine Receptor Antagonists 6 and 7

parameter ^a	value for 6	value for 7
ClogP	2.4	3.4
ClogD _{7.4}	0.03	0.9
MW	322	350
TPSA	32	32
pK _a	9.2	9.2
Early PL Safety Assessment		
in silico PL	90	96
PL MED ^a (μM)	300.0	302.4

^a Calculated physicochemical properties were obtained using standard commercial packages: Biobyte for ClogP calculations, ACD/Labs for ClogD at pH 7.4 and the most basic pK_a. ^a Transformed human liver epithelial cellular phospholipidosis assay measuring phospholipid accumulation per cell. Compounds were classified as positive at the lowest dose for which the induction of phospholipid accumulation was 3-fold over background. MED value is the geometric mean of three independent experiments.

further reduce the pK_a of the basic amine. A second modification made in this template served to compensate for the molecular weight added by the second fluorine atom; we chose to remove the methyl on the amide nitrogen in the expectation that the reduction in molecular weight and increase in polarity (incorporation of one hydrogen bond donor) would provide the maximum benefit with respect to overall physicochemical properties and safety.³³ Through these changes in this design cycle, we identified **6**, one of the clinical candidates (Table 6). Overall, physicochemical properties were optimal from a CNS druglike perspective: ClogP (2.4), ClogD (0.03), MW (322), pK_a (9.2), and TPSA (32). These physicochemical property values are in line with the median values recently reported for a large set of marketed CNS drugs.^{34,48} Lowering the ClogP and pK_a resulted in an improved in silico PL value (90), and the in vitro PL assay value remained high (MED = 300.0 μM). Compound **6** was negative in the Bioluminescence and IVMN assays, and the negative IVMN was confirmed in an exploratory cytogenetics assay.²⁷ All data supported the continued development of **6**. In a 14-day study in rats (4 males/dose), all doses (30, 100, 300 mg/kg) were well tolerated (mean AUC of 189000 ng·h/mL at 300 mg/kg, day 14) and showed no evidence of PL. Treatment-related findings were limited to transient postdose salivation at ≥ 100 mg/kg and a slight decrease in food intake and body weight at 300 mg/kg (≥ 4181 PCEC, Table 11). The only remaining hurdle was demonstration of safety in a second species. The 7-day study in dogs (2/sex) was initiated at 25 mg/kg. Because of convulsions observed on day 3, this dose was lowered on day 4 to 15 mg/kg. There were no treatment-related findings at 15 mg/kg (≥ 1248 PCEC, Table 11). The continual refinement of physicochemical properties, in silico PL value, and in vitro PL value, all while focusing on alignment of drug attributes (potency, specificity, ADME, and safety profile) yielded a compound that moved forward into drug development; **6** has successfully completed regulatory toxicology

Table 7. In Vitro Receptor Binding Affinity

compd	human H ₃		rat H ₃		species ratio
	pK _i ± SEM ^a		pK _i ± SEM ^a		
	(K _i in M)	K _i (nM)	(K _i in M)	K _i (nM) ^b	
1	8.88 ± 0.25	1.3	8.03 ± 0.07	9.3	7
2	8.66 ± 0.10	2.2	8.11 ± 0.05	7.7	3.5
3	8.06 ± 0.11	8.7		82	9.4
4	7.89 ± 0.06	14	6.81 ± 0.05	160	11
5	8.40 ± 0.09	4	7.22 ± 0.06	59	15
6	8.64 ± 0.09	2.3	7.43 ± 0.05	37	16
7	8.84 ± 0.08	1.4	7.73 ± 0.09	19	14

^aData are expressed as geometric mean ± SEM (at least three determinations except for rat K_i of 3 which was N = 1). ^bRat K_i was determined in rat brain for compound 1. All other compounds were tested in HEK-293 cells expressing rat H₃ receptor.

Table 8. Whole Cell Assay, H₃ Receptor cAMP, β-Lactamase Functional Affinity^a

compd	human H ₃		rat H ₃		species ratio
	pK _i ± SEM	K _i	pK _i ± SEM	K _i	
	(K _i in M)	(nM)	(K _i in M)	(nM)	
2	9.05 ± 0.23	0.89	8.45 ± 0.07	3.5	3.7
3	7.93 ± 0.33	12.0		79	6.5
4	8.48 ± 0.08	3.3	7.68 ± 0.29	21	6.4
5	8.83 ± 0.12	1.5	7.69 ± 0.05	21	14
6	8.77 ± 0.10	1.7	8.05 ± 0.07	8.9	5.2
7	8.98 ± 0.09	1.2	8.10 ± 0.11	7.9	6.6

^aData are expressed as geometric mean ± SEM (at least three determinations except for compound 3, which was tested only once in the rat functional assay).

Table 9. Pharmacokinetic (PK) Properties of Compound Set

parameter	2	3	4	5	6	7
Caco-2 AB × 10 ⁻⁶ (cm/s) ^a	8.2	32.5	53.4	34.3	44.7	38.8
HLM T _{1/2} (min) ^b	>120	>120	>120	>120	>120	>120
HLM CL _h (mL min ⁻¹ kg ⁻¹) ^c	<8	<8	<8	<5	<5	<5
P-gp ER ^d	0.95	0.90	1.27	1.29	1.1	0.96
plasma protein binding (f _u) (rat)	0.72	0.47		0.70	0.70	0.56
brain/plasma (rat) (1 h, sc)					2.1	
F (rat) %				24.6	25.9	20.2

^aMS-based quantification of apical → basolateral transfer rate of a test compound at 2 μM across contiguous monolayers of Caco cells.

^bDerived from human liver microsomes. ^cMicrosomal unbound intrinsic clearance using human liver microsomes and an in silico model estimate for f_{u,mic}. ^dRatio of (basal → apical) to (apical → basal) transfer rate of a test compound at 2 μM across contiguous monolayers of MDR1-transfected MDCK cells.

studies and phase I studies including safety, tolerability, and proof of mechanism (POM) (results will be communicated separately). The drive for a best-in-class molecule resulted in the identification of an ideal molecule to broaden the scope of clinical testing. The profile of 6 makes it a practical tool to test not only the primary hypothesis around ADHD but several clinical hypotheses

Table 10. In Vitro PL Values for H₃ Antagonists

compd	mean (μM) ^a	standard		
		deviation (μM)	lower ^b (μM)	upper ^b (μM)
1	17.6	11.2	9.3	25.9
2	37.5	24.6	19.3	55.7
3	119.5	73.9	64.8	174.2
4	245.3	135.9	144.5	346.0
5	300.0	0.01	300.01	300.03
6	300.0	0.3	299.8	300.2
7	302.4	91.4	234.7	370.1

^aAt least three determinations. ^b95% confidence limits.

around antagonism of the histamine H₃ receptor, including the treatment of allergic rhinitis, narcolepsy, and Alzheimer's disease (results will be communicated separately). For clinical study design details of 6, see ClinicalTrials.gov (<http://clinicaltrials.gov/ct2/results?term=pf-03654746>). To further increase our odds of identifying a drug, we continued to probe this highly desirable drug space in an effort to identify a second high-quality clinical candidate. The second clinical candidate, 7, was discovered during follow-up work on the 6 template (Table 6). Compound 7 also has full alignment of the desired attributes (potency, pharmacokinetics, and safety) and large safety multiples over the PCEC in both preclinical species profiled (Table 7–11). While 6 and 7 are structurally similar, they differ in projected human pharmacokinetics, where 7 was projected to have a longer T_{1/2} (~16 h), and in vivo biological profiles (details to be described elsewhere). Further, 7 has successfully completed regulatory toxicology studies and phase I studies including safety and tolerability (results will be communicated separately). For clinical study design details of 7, see ClinicalTrials.gov (<http://clinicaltrials.gov/ct2/results?term=pf-03654764>).

CONCLUSION

There are numerous obstacles along the drug discovery process, some of which slow and can even stop the development of a compound or drug target. Unexpected findings such as phospholipidosis, cardiomyocyte vacuoles, in vitro micronucleus, or unusual structure–activity relationships must be treated as information to be exploited in crafting the next design hypothesis. We have developed a design strategy that leverages medicinal chemistry knowledge, in conjunction with an in silico PL tool and an early in vitro safety PL assay, to identify increasingly safer H₃ receptor antagonists that possess fully aligned attributes (potency, pharmacokinetics, and safety). Critical to the success in identifying compounds free of PL was identifying compounds with PL MED > 200 μM and in silico PL of <98. Drug candidates 6 and 7 met or exceeded all of our design and biological screening criteria and effortlessly moved through both early safety studies and regulatory toxicology studies. The path to these clinical candidates was not a smooth one, but each step of the way generated additional knowledge that was applied in the next design cycle.

In Vitro Pharmacology of Compounds. H₃ receptor binding affinities were determined by displacement of specific ³H-N-α-methylhistamine binding to H₃ receptor binding sites in HEK-293 cells expressing full-length human or rat H₃ receptors. Clinical compounds 6 and 7 bound with high affinity to the human H₃ receptor and with lower affinity to the rat H₃ receptor (Table 7), in addition to having >1000-fold selectivity versus other human

Table 11. In Vivo Assessment of H₃ Antagonist Lead Compounds and Clinical Candidates

compd	maximum tolerated dose (mg/kg)	study duration (days)	human protein binding (hf _u)	projected human PCEC, C _p , nM ^a	species C _{max} ^a (ng/mL) ^b	species C _{max} (nM) ^c	species AUC _(0–24) (ng·h/mL)	safety margin × PCEC ^d
Rat Exploratory Toxicology Studies ^e								
2	≥5	4	0.78	8.5	95 ± 100	302	1245 ± 659	≥35
2	≥30	14	0.78	8.5	1573 ± 189	5002	15513 ± 1451	≥588
3	≥5	14	0.44	59.3	130 ± 141	402	1278 ± 260	≥7
4	≥300	14	0.24	175	2107 ± 803	6292	4444 ^c	≥36
5	≥100	14	0.57	21	2482 ^c	7794	12700 ^c	≥371
6	≥300	14	0.66	10.4	14020 ± 2087	43486	189000 ^c	≥4181
7	≥300	14	0.34	12.3	8057 ± 3083	22990	67400 ^f	≥1869
Dog Exploratory Toxicology Studies ^g								
2	<10	7	0.78	8.5	46.7 ± 0.9	148.5	740 ± 167	<17
3	ND ^h	ND ^h	0.44	59.3	ND ^h	ND ^h	ND ^h	ND ^h
4	<30	7	0.24	175	1717 ± 295	5127	2911 ± 626	<29
5	≥25	7	0.57	21	5197 ± 635	16320	10780 ± 1368	≥777
6	≥15	7	0.66	10.4	4185 ± 1762	12980	18910 ± 10775	≥1248
7	≥15	7	0.34	12.3	6302 ± 1370	17982	18175 ± 222	≥1462

^a Human projected clinical efficacious concentration (PCEC) was calculated ($3 \times$ human H₃ binding K_i) and converted to total plasma concentration (C_p) using measured human plasma protein binding (hf_u). ^b T_{max} ≈ 0.5–1 h postdose. ^c Mean value. ^d Average multiples over the projected clinical efficacious concentrations in the species examined at C_{max} of maximum tolerated dose (corrected for species differences in plasma protein binding). ^e Rat oral exploratory toxicology study (ETS) study. ^f Day 1 value. ^g Dog oral 7 day ETS. ^h ND = not determined.

histamine receptor subtypes (H₁, H₂, and H₄). Compounds 6 and 7 displayed >1000-fold selectivity versus other G-protein-coupled receptors (GPCRs) and transporters.

Clinical candidates 6 and 7 displayed potent antagonist properties in functional assays measuring cAMP utilizing a reporter gene assay (β -lactamase) in HEK293 cells stably expressing full-length human or rat H₃ receptors (Table 8). Results were consistent with the species differences observed in the binding assays.

Pharmacokinetic (PK) Properties of Compound Set (2, 3, 4, 5, 6, and 7). Compounds 6 and 7 both possessed excellent ADME properties (Table 9). Both compounds were well absorbed, as evidenced by both their in vitro properties (Caco-2 A → B, $>38 \times 10^{-6}$ cm/s) and the results of in vivo studies suggesting complete absorption. The blood–brain barrier penetration was specifically tested with 6 (considered representative of the two), and the results indicated that the compound readily penetrated into the brain (brain/plasma ratio of 2.1), with no evidence for efflux mechanisms moderating its central disposition (MDR1 BA/AB = 1.1). In human hepatic microsomes, both compounds were metabolically stable (HLM T_{1/2} > 120 min) and were predicted to have low clearance (<5 mL min^{−1} kg^{−1}) in humans.

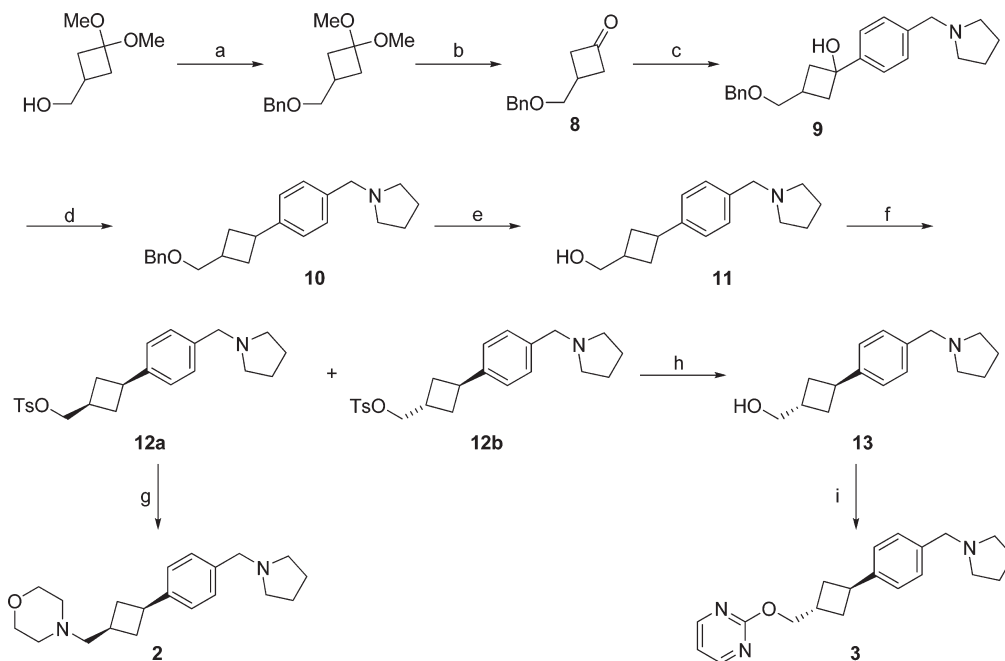
CHEMISTRY

The synthesis of the H₃ receptor antagonists 2 and 3 is outlined in Scheme 1. The preparation of these lead compounds began with etherification of (3,3-dimethoxycyclobutyl)methanol⁴⁹ using benzyl bromide and potassium *tert*-butoxide to afford the corresponding benzyl ether. Unmasking of the latent ketone was accomplished with aqueous *p*-toluenesulfonic acid, generating 8. Lithium–halogen exchange was carried out on 1-(4-bromobenzyl)pyrrolidine via treatment with *n*-butyllithium; reaction with ketone 8 produced carbinol 9 as a mixture of *cis* and *trans* isomers. Access to cyclobutane 10, as a mixture of isomers, was achieved by dehydroxylation of 9 with TFA and triethylsilane.

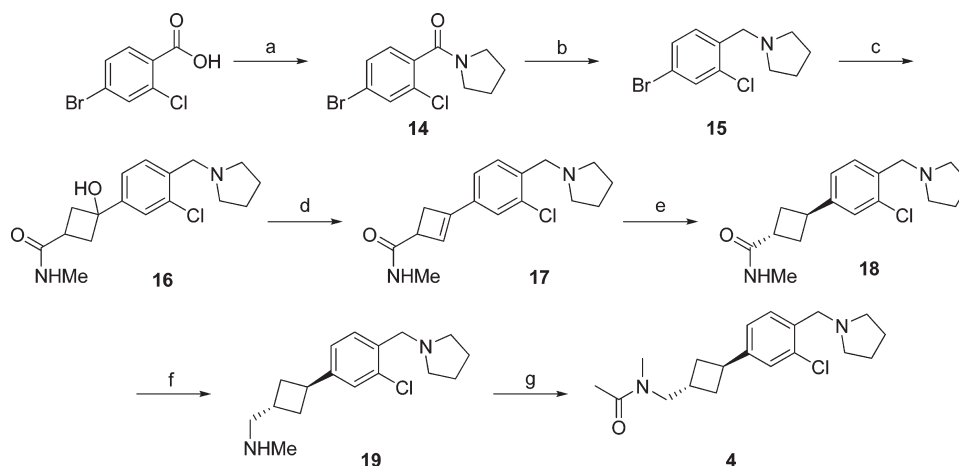
Selective deprotection of the benzyl ether via palladium black catalyzed hydrogenolysis transformed 10 into alcohol 11, which was converted to a mixture of the corresponding *cis* and *trans* tosylates 12a and 12b, respectively. At this stage, the isomers were separated by chromatography. When heated to 120 °C with morpholine in dimethylacetamide, *cis*-tosylate 12a provided compound 2 in moderate yield. Detosylation of *trans*-tosylate 12b was accomplished by heating with magnesium turnings in methanol to give alcohol 13. S_NAr reaction of 2-chloropyrimidine with the potassium alkoxide of 13 generated pyrimidine 3 in good yield.

The synthesis of *exo*-amide H₃ receptor antagonist 4 is depicted in Scheme 2. Pyrrolidine amide 14 was prepared in excellent yield via coupling of 4-bromo-2-chlorobenzoic acid and pyrrolidine using propylphosphonic anhydride (T3P). Subsequent reduction of the amide with borane–THF yielded benzylic amine 15. The conversion of 15 into 16 began with the selective bromine–metal exchange of 15 with *n*-BuLi at −78 °C. An amount of 2 equiv of this lithiated intermediate was added to 3-oxocyclobutanecarboxylic acid, and the resultant cyclobutanecarboxylic acid carbinol was treated in situ with methylamine and T3P to provide amide 16. Dehydration with TFA afforded olefin 17, which was directly hydrogenated using Wilkinson's catalyst to predominantly yield *trans*-cyclobutylamide 18. The *trans* selectivity is presumed to have arisen from a coordination effect between the carbonyl group of the amide and the metal of the Wilkinson's catalyst, as suggested by Schultz and McCloskey for similar hydrogenations of amido-substituted cyclohexanes using Crabtree's catalyst.⁵⁰ Borane–THF reduction of amide 18 gave amine 19, which was acetylated with acetic anhydride to afford H₃ receptor antagonist 4 in high yield.

Synthesis of the *endo*-amide H₃ receptor antagonist 5 is described in Scheme 3. Nucleophilic displacement of 4-bromo-2-fluorobenzyl bromide with pyrrolidine generated benzylic amine 20 in high yield. Selective lithiation of 20 using *n*-BuLi

Scheme 1. Synthesis of Lead Compounds 2 and 3^a

^a Reagents and conditions: (a) KO-*t*-Bu, benzyl bromide, THF, rt (69%); (b) *p*-TsOH (cat.), acetone/water, 65 °C (58%); (c) (i) 1-(4-bromobenzyl)pyrrolidine, *n*-BuLi, THF, -78 °C, (ii) 8, THF, -78 °C (71%); (d) triethylsilane, TFA, 75 °C (taken on crude); (e) palladium black, 45 psi of H₂, EtOH, rt (two steps, 79%); (f) *p*-toluenesulfonyl chloride, pyridine, CH₂Cl₂, 0 °C to rt (93%); (g) 12a, morpholine, DMA, 120 °C (61%); (h) 12b, Mg turnings, MeOH, rt (73%); (i) KO-*t*-Bu, THF, 2-chloropyrimidine, rt (89%).

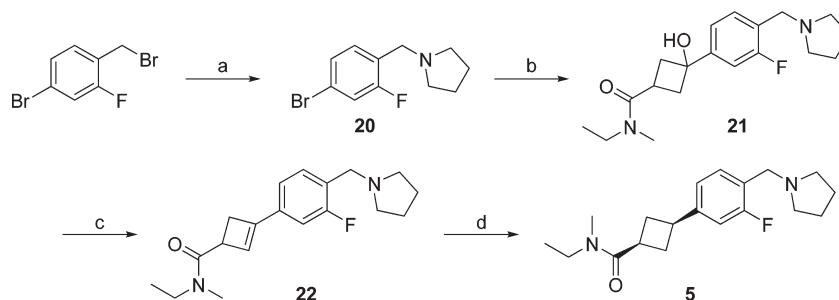
Scheme 2. Synthesis of Lead Compound 4^a

^a Reagents and conditions: (a) T3P, pyrrolidine, EtOAc, rt (96%); (b) BH₃·THF, THF, rt (74%); (c) (i) *n*-BuLi, 3-oxocyclobutanecarboxylic acid, THF, -78 °C to rt; (ii) T3P, CH₃NH₂, rt (48%); (d) TFA, DCE, 75 °C (taken on crude); (e) Rh(Ph₃P)₃Cl, H₂ (45 psi), EtOH, 60 °C (two steps, 37%); (f) BH₃·THF, THF, 70 °C (77%); (g) Ac₂O, Et₃N, CH₂Cl₂, 0 °C (>95%).

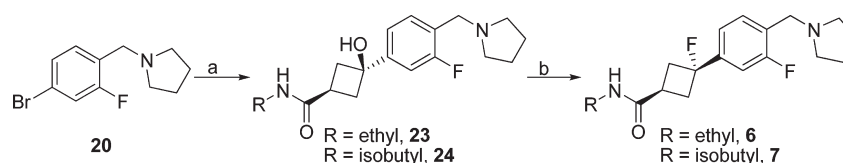
under cryogenic conditions and use of the optimized conditions described in Scheme 2 afforded carbinol 21. Dehydration of 21 afforded cyclobutene 22, which was not stable to column chromatography and was used without further purification. Reduction of the double bond was accomplished via hydrogenation; using 10% Pd/C as catalyst in the presence of hydrogen yielded the desired *cis*-cyclobutane 5 in good yield over two steps.

The syntheses of the two clinical H₃ receptor antagonists, 6 and 7, consisted of three linear steps from 20 (Scheme 4) and

leveraged a late coupling step to install diversity (ethyl or isobutyl). Overall, the synthesis was efficient, requiring only two reaction vessels to complete the process. In the first reaction vessel all the requisite carbons were installed. Aryl bromide 20 was lithiated and added to a precooled solution of 3-oxocyclobutanecarboxylic acid in THF. The resulting cyclobutanecarboxylic acid carbinol was converted to the requisite amide using the coupling reagent T3P and appropriate amine (ethyl or isobutyl) to yield carbinols 23 or 24, respectively. Conversion of the alcohol group to a fluorine was

Scheme 3. Synthesis of Compound 5^a

^a Reagents and conditions: (a) pyrrolidine, CH₃CN, 10 °C to rt (90%); (b) (i) *n*-BuLi, 3-oxocyclobutanecarboxylic acid, THF, −78 °C, (ii) ethylmethylamine, T3P, EtOAc, rt (60%); (c) TFA, CH₂Cl₂, reflux (taken on crude); (d) 10% Pd/C, H₂ (45 psi), EtOH, rt (two steps, 71%).

Scheme 4. Synthesis of Clinical Candidates 6 and 7^a

^a Reagents and conditions: (a) (i) *n*-BuLi, 3-oxocyclobutanecarboxylic acid, THF, −78 °C, (ii) ethylamine or isobutylamine, T3P, EtOAc, rt (R = ethyl, 49%; R = isobutyl, 63%); (b) BAST, CH₂Cl₂, −78 °C (R = ethyl, 58%; R = isobutyl, 85%).

accomplished using the fluorinating agent BAST (bis(2-methoxyethyl)aminosulfur trifluoride). Thus, reaction of carbinols **23** and **24** with BAST afforded **6** and **7**, respectively, with high trans selectivity. We hypothesize that the observed selectivity was imparted either through a stabilized carbocation or simply as a result of a steric interaction that caused the fluorinating reagent to approach the face opposite the carbonyl. Removal of the minor isomers was achieved by either preparative chromatography of the free base or recrystallization of the HCl salt.

Through extensive salt evaluation, we discovered that the tosylate salt possessed optimal properties and this form of **6** was evaluated to determine its acceptability for tablet development. The material was determined to be a crystalline nonsolvated monotosylate salt with a melting onset temperature of 165 °C. Analysis of the moisture sorption isotherm at 25 °C, collected using the kinetic vacuum method, indicated that this solid-state form is nonhygroscopic. Compound **6** tosylate salt has a solubility of greater than 10 mg/mL in 0.1 M phosphate-buffered saline (final pH 7) and a solubility of 23.6 mg/mL in unbuffered water (final pH 3.8). The solubility in 0.1 M phosphate-buffered saline containing 0.5% sodium taurocholate/pamitoyllecylphosphatidylcholine salts (final pH 6.5) was determined to be greater than 11 mg_A/mL (active component). The apparent solubility of the **6** tosylate salt in simulated gastric fluid (pH 1) was greater than 15 mg/mL (active component). Overall, the high aqueous solubility of this compound in all simulated biological media suggests that the candidate would remain well solubilized in the gastrointestinal tract.

MATERIALS AND METHODS

Physicochemical Property Data. This analysis included calculated lipophilicity (ClogP), calculated lipophilicity at pH 7.4 (ClogD), molecular weight (MW), topological polar surface area (TPSA), the

number of hydrogen bond donors (HBD), and the calculated most basic center (pK_a). Calculated physicochemical properties were obtained using standard commercial packages: Biobyte for ClogP calculations and ACD/Labs for ClogD at pH 7.4 and the most basic pK_a. TPSA was calculated using the method developed by Ertl.⁵¹

Chemistry. General Information. All solvents and reagents were obtained from commercial sources and were used as received. All reactions were followed by TLC (TLC plates F254, Merck) or LCMS (liquid chromatography–mass spectrometry) analysis. Proton and ¹³C NMR spectra were obtained using deuterated solvent on a Varian 300, 400, or 500 MHz instrument. All proton shifts are reported in δ units (ppm) downfield of TMS (tetramethylsilane) and were measured relative to the signals for chloroform (7.27 ppm) and methanol (3.31 ppm). All ¹³C shifts are reported in δ units (ppm) relative to the signals for chloroform (77.0 ppm) and methanol (49.1 ppm) with ¹H decoupled observation. All coupling constants (*J*) are reported in hertz (Hz). NMR abbreviations are as follows: app, apparent; br, broadened; s, singlet; d, doublet; t, triplet; q, quartet; p, pentuplet; m, multiplet; dd, doublet of doublets; ddd, doublet of doublet of doublets; sept, septuplet. GCMS data were recorded on an HP 6890 GC system equipped with a 5973 mass selective detector (stationary phase, HP-1, fused silica, 12 m × 0.202 mm, 0.33 μm; temperature limits of −60 to 325 °C; ramp rate of 30 °C/min; solvent delay = of 0.4 min). Analytical analyses by Ultra performance liquid chromatography (UPLC) were performed on a Waters Acquity system with PDA detection (UV 210 nm) at 45 °C, flow rate of 0.5 mL/min, with a gradient of 95/5 buffer/acetonitrile (0–7.55 min), 10/90 buffer/acetonitrile (7.55–7.85 min), 95/5 buffer/acetonitrile (8.10–10.30 min) using the following columns and buffers: Waters BEH C8 column (2.1 mm × 100 mm, 1.7 μm) with 50 mM sodium perchlorate/0.1% phosphoric acid or 10 mM ammonium bicarbonate as buffer; Waters BEH RP C18 column (2.1 mm × 100 mm, 1.7 μm) or Waters HSS T3 (2.1 mm × 100 mm, 1.8 μm) column with 0.1% methanesulfonic acid buffer. All melting points are uncorrected. Elemental analyses were performed by QTI Development. Mass spectra were recorded on a Micromass ADM atmospheric pressure chemical

ionization instrument (APCI). High resolution mass spectra were obtained on an Agilent LCMS TOF instrument equipped with a Zorbax Eclipse column (50 mm \times 4.6 mm, 1.8 μ m XDB-C18) using 0.1% aqueous formic acid as mobile phase A1 and acetonitrile containing 0.1% formic acid as mobile phase B1. Column chromatography was carried out on silica gel 60 (32–60 mesh, 60 Å) or on prepacked Biotage columns. The purities of final compounds 2–7 as measured by UPLC and/or elemental analysis methods were found to be above 95%.

4-({cis-3-[4-(Pyrrolidin-1-ylmethyl)phenyl]cyclobutyl}-methyl)morpholine (2). Morpholine (33.6 mL, 385 mmol) was added to **12a** (76.3 g, 191 mmol) in dimethylacetamide (DMA) (191 mL), and the mixture was heated at 120 °C for 1 h. The mixture was cooled to room temperature and concentrated. EtOAc and concentrated HCl (32 mL) were added. Solvents were removed in vacuo and two additional portions of EtOAc were added followed by reconcentration to help remove residual DMA. EtOAc (600 mL) was added to the resulting residue, and stirring was continued for 2 days. The solvent was decanted off, and the gummy residue was dissolved in 3:1 CHCl₃/MeOH and basified with 15% aqueous NaOH. The organic layer was concentrated and purified by chromatography using a gradient of 3–50% MeOH in CH₂Cl₂ containing 0.3% NH₄OH, affording the title compound (36.8 g, 61%) as a solid. This was dissolved in EtOAc, treated with 1 N HCl in THF, and filtered to yield the HCl salt as a white solid. ¹H NMR (MeOH-*d*₄, 400 MHz) δ 7.42 (AB quartet, $\Delta\nu_{AB}$ = 50.7, J_{AB} = 8.3, 4H), 4.35 (s, 2H), 4.03 (dd, J = 12.9, 3.7, 2H), 3.84 (ddd, J = 13.3, 13.3, 1.7, 2H), 3.49–3.59 (m, 1H), 3.45 (br d, J = 12.0, 4H), 3.28 (d, J = 7.1, 2H), 3.13–3.22 (m, 4H), 2.77–2.87 (m, 1H), 2.61–2.68 (m, 2H), 2.10–2.22 (m, 2H), 1.96–2.05 (m, 4H). ¹³C NMR (MeOH-*d*₄, 100 MHz) δ 146.7, 130.4, 128.8, 127.2, 63.8, 62.0, 57.7, 53.5, 51.9, 36.5, 34.6, 26.5, 22.6. HRMS m/z , calcd (M + 1) 315.2430, observed 315.2442.

2-({trans-3-[4-(Pyrrolidin-1-ylmethyl)phenyl]cyclobutyl}-methyl)pyrimidine (3). Potassium *tert*-butoxide (1.0 M in THF, 22.0 mL, 22.0 mmol) was added to a solution of **13** (3.6 g, 14.7 mmol) and 2-chloropyrimidine (1.85 g, 16.2 mmol) in THF (14 mL) to give a cloudy, dark pink mixture. After 10 min, saturated aqueous NH₄Cl was added and the mixture was extracted with 3:1 CHCl₃/*i*-PrOH. The organic layers were concentrated to give 5.2 g of the crude title compound. Chromatography using a gradient of 3–8% MeOH in CH₂Cl₂ containing 0.2% NH₄OH yielded the title compound (4.2 g, 89%) as a semisolid. The besylate salt was prepared in MeOH using 1 equiv of benzenesulfonic acid to yield 6.4 g of a light yellow solid. A portion of this material was recrystallized from water to provide an analytical sample. ¹H NMR (MeOH-*d*₄, 400 MHz) δ 8.58 (d, J = 4.6, 2H), 7.81–7.83 (m, 2H), 7.37–7.45 (m, 7H), 7.10 (t, J = 5.0, 1H), 4.56 (d, J = 7.1, 2H), 4.33 (s, 2H), 3.76 (tt, J = 8.6, 8.2, 1H), 3.42–3.50 (m, 2H), 3.13–3.31 (m, 2H), 2.75–2.87 (m, 1H), 2.31–2.42 (m, 4H), 2.08–2.22 (m, 2H), 1.90–2.06 (m, 2H). ¹³C NMR (MeOH-*d*₄, 100 MHz) δ 166.6, 160.9, 149.7, 146.5, 131.7, 131.4, 129.7, 129.5, 128.6, 127.1, 116.6, 72.1, 59.2, 54.9, 37.7, 32.2, 31.4, 23.9. HRMS m/z , calcd (M + 1) 324.2070, observed 324.2062.

N-({trans-3-[3-Chloro-4-(pyrrolidin-1-ylmethyl)phenyl]cyclobutyl}methyl)-*N*-methylacetamide (4). Acetic anhydride (9.2 mL, 97 mmol) was added to a 0 °C solution of **19** (23.7 g, 81.2 mmol) and Et₃N (22.6 mL, 162 mmol) in CH₂Cl₂ (230 mL). After the mixture was stirred for 30 min, 1 N aqueous NaOH (200 mL) was added and the phases were separated. The aqueous phase was extracted twice with EtOAc, and the combined organics were dried over MgSO₄, filtered, and concentrated to yield 29.2 g of crude product. Chromatography using a gradient of 5–20% MeOH in CH₂Cl₂ containing 0.1% NH₄OH yielded the title compound (27 g, 99%) as a colorless, viscous oil. This was dissolved in EtOAc (200 mL) and treated with 2 M HCl in Et₂O (81.2 mL) to afford the mono-HCl salt of the title compound as a

white solid (30.6 g, 99%). ¹H NMR (MeOH-*d*₄, 400 MHz) δ 7.70–7.73 (m, 1H), 7.50 and 7.46 (2 d, J = 1.7, 1H total), 7.40 and 7.36 (2 dd, J = 7.9, 1.5, 1H total), 4.57 (s, 2H), 3.70–3.82 (m, 3H), 3.53–3.60 (m, 2H), 3.24 (m, 2H), 3.24 and 3.14 (2 s, 3H total), 2.72–2.86 (m, 1H), 2.17–2.38 (m, 9H), 2.02–2.12 (m, 2H). ¹³C NMR (MeOH-*d*₄, 100 MHz) δ 175.7, 175.4, 151.6, 151.5, 136.2, 134.3, 129.4, 129.3, 127.6, 127.5, 127.4, 127.3, 57.1, 55.9, 55.2, 54.7, 38.3, 37.2, 37.0, 36.0, 32.8, 32.6, 31.0, 30.4, 24.0, 20.2, 19.8. HRMS m/z , calcd (M + 1) 335.1884, observed 335.1880.

cis-N-Ethyl-3-[3-fluoro-4-(pyrrolidin-1-ylmethyl)phenyl]-N-methylcyclobutanecarboxamide (5). Following the general procedure described for preparing olefin **17**, compound **21** (71.76 g, 214.6 mmol) yielded 182.0 g of crude olefin **22** as the TFA salt, *N*-ethyl-3-[3-fluoro-4-(pyrrolidin-1-ylmethyl)phenyl]-*N*-methylcyclobut-2-ene-1-carboxamide, as a brown oil. This was dissolved in EtOH (1.5 L) and hydrogenated (~45 psi) with 10% Pd/C (10 g) at room temperature for 1.5 h. After filtration and concentration, the resulting oil was dissolved in EtOAc (500 mL), washed with a solution of K₂CO₃ (60 g) in water (400 mL), then with brine (200 mL), and dried over MgSO₄. Filtration and concentration afforded 66.26 g of an orange oil, which was purified by chromatography, flushing first with CH₂Cl₂ and then eluting with 5% MeOH in CH₂Cl₂ to yield 41.75 g (58%) of pure title compound and 9.98 g (14%) of ~85–90% pure material. The cleaner material (41.75 g, 131.1 mmol) was dissolved in EtOAc (1 L); 2 N HCl in Et₂O (80 mL, 160 mmol) was added over ~1 min with vigorous stirring. After 30 min, the light orange precipitate was collected, rinsed with EtOAc, and dried to yield the corresponding HCl salt of **5** (36.15 g). A portion was recrystallized from MeOH/EtOAc to provide an analytical sample as a white solid, mp 196–196.5 °C. ¹H NMR (300 MHz, CDCl₃) δ 7.79 (t, J = 7.9, 1H), 7.07–7.00 (m, 2H), 4.20 (d, J = 5.4, 2H), 3.57–3.64 (m, 2H), 3.47–3.53 (m, 2H), 3.16–3.30 (m, 2H), 2.91 and 2.88 (2 s, 3H total), 2.79–2.85 (m, 2H), 2.50–2.60 (m, 2H), 2.34–2.46 (m, 2H), 2.14–2.26 (m, 2H), 1.95–2.06 (m, 2H), 1.14 and 1.07 (2 t, J = 7.1, 3H total). ¹³C NMR (100 MHz, CDCl₃) δ (mixture of rotamers) 173.3, 162.7, 160.2, 150.6, 150.5, 133.6, 133.6, 124.0, 124.0, 114.4, 114.3, 114.0, 113.8, 52.6, 49.9, 49.9, 44.1, 42.7, 35.3, 34.3, 33.5, 32.8, 32.4, 23.2, 14.1, 12.4. HRMS m/z , calcd (M + 1) 319.2180, observed 319.2188. Anal. Calcd for C₁₉H₂₇FN₂O·HCl: C, 64.30; H, 7.95; N, 7.89. Found: C, 64.36; H, 8.02; N, 7.97.

trans-N-Ethyl-3-fluoro-3-[3-fluoro-4-(pyrrolidin-1-ylmethyl)phenyl]cyclobutanecarboxamide (6). A solution of **23** (48.7 g, 152.0 mmol) in CH₂Cl₂ (450 mL) was added over 50 min down the reaction flask walls to a –78 °C solution of bis(2-methoxyethyl)aminosulfur trifluoride (BAST) (42.0 mL, 227.8 mmol) in CH₂Cl₂ (375 mL). After 2.5 h at –78 °C, the cooling bath was removed and the mixture was stirred for 16 h at room temperature. With stirring, aqueous NaHCO₃ was carefully added in portions until all foaming subsided. Solid K₂CO₃ was then added to ensure that the pH was >8. The phases were separated, and the aqueous phase was extracted with additional CH₂Cl₂ (2 \times 100 mL). The organic phases were combined, dried over MgSO₄, filtered, and concentrated to yield a dark orange-brown oil (50.2 g). This crude material was purified by chromatography, eluting with EtOAc and 10% MeOH/EtOAc to yield 28.21 g (58%) of the title compound. The monotosylate salt of **6** was prepared by addition of a solution of *p*-toluenesulfonic acid (2.50 g, 13.14 mmol) in EtOAc (70 mL) to a stirring solution of the free base (4.18 g, 13.0 mmol) in EtOAc (35 mL). The resulting mixture was stirred for an additional hour. The white precipitate was filtered, rinsed with EtOAc, and air-dried to afford 6.32 g of the tosylate salt of **6**. This material was dissolved in MeOH, filtered to remove particulates, and reconcentrated. The resulting solid was dissolved in ~12–14 mL of MeOH with gentle heating. EtOAc (75 mL) was added over 20 min, and then the mixture was stirred for 1 h at room temperature. The solid was filtered, rinsed with EtOAc, and air-dried to yield the monotosylate salt of **6** (5.59 g) as a white, crystalline powder.

^1H NMR (CDCl_3) δ 7.71 (d, J = 8.3, 2H), 7.65 (t, J = 7.9, 1H), 7.28–7.22 (m, 2H), 7.15 (d, J = 7.9, 2H), 6.52 (br s, 1H), 4.28 (d, J = 5.4, 2H), 3.68–3.37 (m, 2H), 3.33–3.18 (m, 3H), 2.97–2.88 (m, 2H), 2.84–2.57 (m, 4H), 2.32 (s, 3H), 2.27–1.96 (m, 4H), 1.07 (t, J = 7.3, 3H). ^{13}C NMR (CDCl_3) δ 173.5, 161.0 (dd, $J_{\text{C-F}}$ = 248.9, 1.5), 147.0 (dd, $J_{\text{C-F}}$ = 23.6, 7.4), 142.0, 140.1, 133.3 (d, $J_{\text{C-F}}$ = 3.0), 128.8, 125.8, 121.5 (dd, $J_{\text{C-F}}$ = 8.8, 3.7), 116.1 (dd, $J_{\text{C-F}}$ = 14.7, 1.5), 112.6 (dd, $J_{\text{C-F}}$ = 23.6, 8.8), 96.4 (dd, $J_{\text{C-F}}$ = 197.6, 2.2), 53.2, 50.4 (d, $J_{\text{C-F}}$ = 2.9), 38.6 (d, $J_{\text{C-F}}$ = 24.3), 34.4, 32.4, 22.7, 21.3, 14.7. Anal. Calcd for $\text{C}_{18}\text{H}_{24}\text{F}_2\text{N}_2\text{O} \cdot \text{C}_7\text{H}_8\text{O}_3\text{S}$: C, 60.71; H, 6.52; N, 5.66; F, 7.68; S, 6.48. Found: C, 60.55; H, 6.40; N, 5.58; F, 7.67; S, 6.68. HRMS m/z , calcd ($M + 1$) 323.1929, observed 323.1934.

trans-3-Fluoro-3-[3-fluoro-4-(pyrrolidin-1-ylmethyl)phenyl]-N-(2-methylpropyl)cyclobutanecarboxamide (7). The free base of this material was prepared in 85% yield as a waxy orange solid following the general procedure described for compound 6 and substituting 24 for 23. The free base 7 (13.8 g, 79.0 mmol) was dissolved in EtOAc (250 mL) and treated with *p*-toluenesulfonic acid (15.2 g, 79.9 mmol) in EtOAc (150 mL). The resulting solution was stirred overnight, and the white precipitate was collected and dried under nitrogen purge to yield 16.5 g of the monotosylate salt. The salt was dissolved in a mixture of MeOH (20 mL) and EtOAc (40 mL) by application of heat. Following filtration through a nylon filter, EtOAc (250 mL) was added to the filtrate over ~40 min. After the mixture was stirred for an additional hour, the resulting white solid was collected and dried under nitrogen purge. This recrystallization procedure was repeated twice to afford 12.2 g of the tosylate salt of 7 as a solid. ^1H NMR (300 MHz, CDCl_3) δ 11.36 (br s, 1H), 7.79–7.74 (m, 3H), 7.32–7.28 (m, 2H), 7.19 (d, J = 7.9, 2H), 5.78 (br s, 1H), 4.32 (d, J = 5.4, 2H), 3.79–3.73 (m, 2H), 3.29 (tt, J = 8.7, 8.3, 1H), 3.09 (dd, J = 7.1, 6.3, 2H), 2.93–2.66 (m, 6H), 2.36 (s, 3H), 2.24–2.18 (m, 2H), 2.08–2.02 (m, 2H), 1.76 (sept, J = 6.7, 1H), 0.89 (d, J = 6.6, 6H). ^{13}C NMR (100 MHz, CDCl_3) δ 174.0, 161.3 (d, $J_{\text{C-F}}$ = 248.0), 147.4 (dd, $J_{\text{C-F}}$ = 24.1, 7.5), 142.5, 140.3, 133.3 (d, $J_{\text{C-F}}$ = 3.0), 128.8, 125.8, 121.5 (dd, $J_{\text{C-F}}$ = 9.0, 4.5), 116.1 (d, $J_{\text{C-F}}$ = 13.5), 112.3 (dd, $J_{\text{C-F}}$ = 24.1, 9.0), 96.7 (d, $J_{\text{C-F}}$ = 196.9), 53.4, 50.0 (d, $J_{\text{C-F}}$ = 3.0), 46.9, 38.6 (d, $J_{\text{C-F}}$ = 25.6), 32.5, 28.4, 22.7, 21.2, 20.0. Anal. Calcd for $\text{C}_{20}\text{H}_{28}\text{F}_2\text{N}_2\text{O} \cdot \text{C}_7\text{H}_8\text{O}_3\text{S}$: C, 62.05; H, 6.94; N, 5.36; F, 7.27; S, 6.14. Found: C, 61.85; H, 7.03; N, 5.32; F, 7.21; S, 6.34. HRMS m/z , calcd ($M + 1$) 351.2242, observed 351.2236.

{[3,3-Dimethoxycyclobutyl)methoxy]methyl}benzene (8a). *t*-BuOK (1 M in THF, 163 mL, 163 mmol) was added at room temperature to a solution of (3,3-dimethoxycyclobutyl)methanol⁵⁰ (11.9 g, 81.5 mmol) in THF (100 mL). The mixture was stirred for 30 min. Benzyl bromide (10.2 mL, 85.6 mmol) was added, and the stirring was continued for an additional 30 min. Water and CH_2Cl_2 were added, and the organic layer was separated, dried over MgSO_4 , filtered, and concentrated. Chromatography using a gradient of 100% hexanes to 5% EtOAc/hexanes furnished the desired product as a colorless oil (13.2 g, 69%). ^1H NMR (CDCl_3 , 400 MHz) δ 7.36–7.25 (m, 5H), 4.52 (s, 2H), 3.48 (d, J = 7.0, 2H), 3.16 (s, 3H), 3.12 (s, 3H), 2.44–2.26 (m, 3H), 1.90–1.84 (m, 2H). ^{13}C NMR (CDCl_3 , 100 MHz) δ 138.8, 128.6, 127.9, 127.8, 101.1, 74.7, 73.2, 48.6, 48.4, 34.9, 24.9. MS (APCI) m/z = 205.3 ($M - \text{OCH}_3$).

3-[(Benzyloxy)methyl]cyclobutanone (8). *p*-Toluenesulfonic acid monohydrate (2.1 g, 11 mmol) was added to a solution of 8a (13.0 g, 55.1 mmol) in acetone/water (3:1, 200 mL). After heating for 45 min at 65 °C, the mixture was cooled to room temperature and concentrated. The residue was dissolved in EtOAc, washed with 5% aqueous NaOH, dried over MgSO_4 , filtered, and concentrated. Chromatography using 10% EtOAc/hexanes yielded the title compound as a colorless oil (6.0 g, 58%). ^1H NMR (CDCl_3 , 400 MHz) δ 7.28–7.38 (m, 5H), 4.56 (s, 2H), 3.59 (d, J = 6.3, 2H), 3.88–3.18 (m, 2H), 2.84–2.92 (m, 2H), 2.64–2.75 (m, 1H). ^{13}C NMR (CDCl_3 , 100 MHz) δ 207.6, 138.3, 128.7, 127.9, 127.8, 73.4, 73.1, 50.2, 23.9. GCMS m/z = 190 (M^+).

3-[(Benzyloxy)methyl]-1-[4-(pyrrolidin-1-ylmethyl)phenyl]-cyclobutanone (9). *n*-BuLi (2.5 M in hexane, 3.2 mL, 8.0 mmol) was slowly added to a –78 °C solution of 1-(4-bromobenzyl)pyrrolidine (1.9 g, 7.9 mmol) in THF (13 mL). After 30 min, a –78 °C solution of 8 (1.0 g, 5.3 mmol) in THF (1 mL) was added via cannula and the resulting solution was stirred at –78 °C for 30 min. The reaction was quenched with saturated aqueous NH_4Cl and diluted with EtOAc. The organics were dried over MgSO_4 , filtered, and concentrated. Chromatography using a gradient of 2% MeOH/ CH_2Cl_2 containing 0.1% NH_4OH to 30% MeOH/ CH_2Cl_2 containing 0.1% NH_4OH afforded the title compound (1.3 g, 71%) as a colorless oil. GCMS analysis indicated a ~3:1 mixture of isomers, presumed to be *cis* and *trans*. ^1H NMR (CDCl_3 , 400 MHz) δ 7.28–7.47 (m, 9H), 4.61 and 4.52 (singlets, 2H total), 3.46–3.62 (m, 4H), 2.75–2.97 (m, 2H), 2.48–2.53 (m, 4H), 2.22–2.47 (m, 4H), 1.75–1.82 (m, 4H). MS (APCI) m/z = 352.4 ($M + 1$).

1-[4-{3-[(Benzyloxy)methyl]cyclobutyl}benzyl]pyrrolidine (10). Triethylsilane (49.0 mL, 308 mmol) and TFA (47 mL, 620 mmol) were added to 9 (21.6 g, 61.5 mmol) and the resulting biphasic mixture was heated at 75 °C for 1 h, cooled to room temperature and concentrated. This material was used without purification in the next step. For characterization, a portion of the crude material was dissolved in EtOAc and washed with 1 N aqueous NaOH, dried over MgSO_4 , filtered and concentrated. Chromatography using EtOAc and 10% MeOH/EtOAc gave a ~1:1 mixture of *cis* and *trans* isomers of the title compound as a colorless oil. ^1H NMR (CDCl_3 , 400 MHz) δ 7.14–7.40 (m, 9H), 4.59 and 4.54 (singlets, 2H total), 3.65 and 3.47 (doublets, J = 7.2 and 6.3, 2H total), 3.60 (singlet, 1H), 3.59 (singlet, 1H), 3.55–3.61 and 3.36–3.43 (multiplets, 1H total), 2.45–2.65 (overlapping multiplets, 6H total), 2.20–2.34 and 1.86–1.94 (multiplets, 3H total), 1.75–1.82 (m, 4H). MS (APCI) m/z = 336.4 ($M + 1$).

{3-[4-(Pyrrolidin-1-ylmethyl)phenyl]cyclobutyl}methanol (11). A sample of 20% palladium black (4.0 g) was added to a stirring solution of crude 10 (61.5 mmol) in EtOH (250 mL). This mixture was hydrogenated at 45 psi for 1 h, filtered through Celite, and concentrated. The residue was dissolved in CH_2Cl_2 and washed with saturated aqueous NaHCO_3 . The aqueous layer was extracted with 3:1 CHCl_3 /*i*-PrOH, and the combined organic layers were dried over MgSO_4 , filtered, and concentrated. Chromatography with a gradient of 2–20% MeOH/ CH_2Cl_2 containing 0.2% NH_4OH provided the desired product as the TFA salt. This was dissolved in 3:1 CHCl_3 /*i*-PrOH and washed with aqueous K_2CO_3 . Removal of solvent yielded the title compound (11.9 g, 79%, colorless oil) as a mixture of *cis* and *trans* isomers, which was used without further separation. ^1H NMR (CDCl_3 , 400 MHz) δ 7.20–7.24 (m, 2H), 7.09–7.14 (m, 2H), 5.69 (br s, 1H), 3.76 and 3.75 (singlets, 2H total), 3.24–3.65 (overlapping doublets and multiplets, 3H total), 2.70–2.77 (m, 4H), 2.30–2.43 (m, 2H), 1.73–1.85 and 2.08–2.16 (overlapping multiplets, 7H total). MS (APCI) m/z = 246.3 ($M + 1$).

{cis-3-[4-(Pyrrolidin-1-ylmethyl)phenyl]cyclobutyl}methyl 4-Methylbenzenesulfonate (12a) and {trans-3-[4-(Pyrrolidin-1-ylmethyl)phenyl]cyclobutyl}methyl 4-Methylbenzenesulfonate (12b). *p*-Toluenesulfonyl chloride (*p*-TsCl) (49.9 g, 262 mmol) was added to a 0 °C solution of 11 (53.5 g, 218.4 mmol) and pyridine (88.3 mL, 1.09 mol) in CH_2Cl_2 (250 mL). After 30 min, an additional portion of *p*-TsCl (10.0 g, 52.5 mmol) was added, and the mixture was stirred overnight at room temperature. The mixture was concentrated to near dryness. Water, CH_2Cl_2 , and solid NaHCO_3 and K_2CO_3 were added, and the mixture was stirred for 90 min to consume excess *p*-TsCl. The organic layer was separated, dried over MgSO_4 , filtered, and concentrated. The resulting oil (110 g) was purified by chromatography using a gradient of 2–5% MeOH in CH_2Cl_2 to provide a 1:2 mixture of *cis* and *trans* isomers of the product (57 g, 66%) as a brown gum. The isomers were separated by preparative HPLC (Chiralpak AD column, eluting with

85/15 heptane/EtOH with 0.1% diethylamine modifier) to afford the following compounds.

12a (cis isomer): colorless gum. ^1H NMR (CDCl_3 , 400 MHz) δ 7.79 (d, J = 8.3, 2H), 7.32 (d, J = 7.9, 2H), 7.24 (d, J = 7.9, 2H), 7.08 (d, J = 7.9, 2H), 3.99 (d, J = 6.2, 2H), 3.57 (s, 2H), 3.31–3.40 (m, 1H), 2.53–2.63 (m, 1H), 2.46–2.50 (m, 4H), 2.42 (s, 3H), 2.36–2.41 (m, 2H), 1.78–1.87 (m, 2H), 1.72–1.77 (m, 4H). ^{13}C NMR (CDCl_3 , 100 MHz) δ 144.4, 143.1, 136.9, 132.8, 129.6, 128.5, 127.5, 125.8, 73.6, 60.0, 53.8, 35.3, 31.9, 29.7, 23.1, 21.3. MS (APCI) m/z = 400.3 ($M + 1$).

12b (trans isomer): colorless gum. ^1H NMR (CDCl_3 , 400 MHz) δ 7.84 (d, J = 8.1, 2H), 7.37 (d, J = 7.8, 2H), 7.26 (d, J = 8.2, 2H), 7.13 (d, J = 8.2, 2H), 4.19 (d, J = 7.4, 2H), 3.59 (s, 2H), 3.49–3.57 (m, 1H), 2.57–2.65 (m, 1H), 2.49–2.52 (m, 4H), 2.47 (s, 3H), 2.23–2.31 (m, 2H), 2.14–2.21 (m, 2H), 1.76–1.80 (m, 4H). ^{13}C NMR (CDCl_3 , 100 MHz) δ 144.7, 143.9, 137.0, 133.2, 129.8, 128.9, 127.9, 126.1, 73.6, 60.3, 54.1, 35.9, 30.6, 29.9, 23.4, 21.6. MS (APCI) m/z = 400.3 ($M + 1$).

{trans-3-[4-(pyrrolidin-1-ylmethyl)phenyl]cyclobutyl}-methanol (13). Magnesium turnings (4.87 g, 201 mmol) and **12b** (8.0 g, 20 mmol) in MeOH (160 mL) were stirred for 4 h to give a milky mixture. Aqueous NaOH (15%) was added, and the mixture was extracted with 3:1 CHCl_3 /*i*-PrOH. The organic phase was dried over MgSO_4 , filtered, and concentrated to yield the title compound (3.6 g, 73%) as a colorless oil. This material was used without further purification. ^1H NMR (CDCl_3 , 400 MHz) δ 7.28 (d, J = 8.0, 2H), 7.19 (d, J = 8.0, 2H), 3.73 (d, J = 7.4, 2H), 3.60 (s, 2H), 3.52–3.58 (m, 1H), 3.47 (br s, 1H), 2.49–2.56 (m, 4H), 2.41–2.49 (m, 1H), 2.16–2.29 (m, 4H), 1.70–1.81 (m, 4H). ^{13}C NMR (CDCl_3 , 100 MHz) δ 144.9, 136.2, 128.9, 126.1, 66.2, 60.2, 53.9, 36.3, 32.8, 31.0, 23.2. MS (APCI) m/z = 246.4 ($M + 1$).

(4-Bromo-2-chlorophenyl)(pyrrolidin-1-yl)methanone (14). T3P (48.6 g, 153 mmol, 50 wt % in EtOAc) was added to a mixture of 4-bromo-2-chlorobenzoic acid (30 g, 130 mmol), triethylamine (25.8 g, 255 mmol), and pyrrolidine (18 g, 255 mmol) in EtOAc (1.5 L). After 1 h, 1 N aqueous NaOH (200 mL) was added and the mixture was stirred for 10 min. The layers were separated, and the aqueous phase was extracted with EtOAc (2×500 mL). The combined organic extracts were dried over MgSO_4 , filtered, and concentrated to provide a viscous oil. Chromatography using a gradient of 50–80% EtOAc in hexanes yielded the title compound as a light yellow, viscous oil (35.4 g, 96%). ^1H NMR (CDCl_3 , 400 MHz) δ 7.56 (d, J = 1.7, 1H), 7.43 (dd, J = 8.3, 1.7, 1H), 7.17 (d, J = 8.3, 1H), 3.63 (br app t, J = 6.6, 2H), 3.17 (br app t, J = 6.6, 2H), 2.00–1.84 (m, 4H). ^{13}C NMR (CDCl_3 , 100 MHz) δ 166.0, 136.6, 132.6, 131.3, 130.7, 128.9, 123.3, 48.0, 45.8, 26.1, 24.7. MS (APCI) m/z = 287.9 ($M + 1$).

1-(4-Bromo-2-chlorobenzyl)pyrrolidine (15). Borane–THF complex (1.0 M in THF, 367 mL, 367 mmol) was added dropwise to a solution of **14** (35.3 g, 122 mmol) in THF (120 mL), and the resulting mixture was stirred at room temperature for 21 h. The reaction was quenched with MeOH (120 mL), and the mixture was heated to 80 °C for 18 h. The mixture was cooled to room temperature and concentrated and the resulting residue was purified by chromatography using 50% EtOAc in hexanes to yield the title compound as a colorless, viscous oil (24.4 g, 74%). ^1H NMR (CDCl_3 , 400 MHz) δ 7.47 (br s, 1H), 7.38–7.33 (m, 2H), 3.66 (s, 2H), 2.58–2.54 (m, 4H), 1.80–1.76 (m, 4H). ^{13}C NMR (CDCl_3 , 100 MHz) δ 136.4, 134.8, 132.0, 131.9, 130.0, 120.7, 56.6, 54.4, 23.8. MS (APCI) m/z = 275.8 ($M + 1$).

3-[3-Chloro-4-(pyrrolidin-1-ylmethyl)phenyl]-3-hydroxy-N-methylcyclobutanecarboxamide (16). *n*-Butyllithium (2.5 M in hexanes, 135 mL, 0.335 mol) was added down the reaction flask walls over 25 min to a –78 °C solution of **15** (92.0 g, 0.335 mol) in THF (400 mL). After the mixture was stirred at –78 °C for 1 h, a –78 °C solution of 3-oxocyclobutanecarboxylic acid (19.0 g, 167.5 mmol) in THF (400 mL) was cannulated into the reaction mixture over 15 min. The resulting dark orange solution was slowly warmed to room temperature over 16 h. To the crude solution of the intermediate 3-[3-chloro-4-(pyrrolidin-1-ylmethyl)phenyl]-3-hydroxycyclobutanecarboxylic acid

were added methylamine (2.0 M in THF, 167 mL, 334 mmol) and T3P (50 wt % solution in EtOAc, 128 mL, 201 mmol). The resulting reaction mixture was stirred at room temperature for 1 h. Then 1 N aqueous NaOH (575 mL) and EtOAc (400 mL) were added and the layers were separated. The aqueous layer was subjected to EtOAc extraction (2×500 mL), and the combined organic layers were dried over MgSO_4 , filtered, and concentrated. Chromatography with a gradient of 5–15% MeOH in CH_2Cl_2 containing 0.25% NH_4OH provided the title compound (25.9 g, 48%). ^1H NMR (CDCl_3 , 400 MHz) δ 7.46–7.48 (m, 2H), 7.34 (dd, J = 7.9, 1.7, 1H), 6.03–6.11 (br m, 1H), 5.77 (br s, 1H), 3.76 (s, 2H), 2.85 (d, J = 4.9, 3H), 2.73–2.86 (m, 3H), 2.56–2.63 (m, 4H), 2.47–2.54 (m, 2H), 1.76–1.84 (m, 4H). ^{13}C NMR (CDCl_3 , 100 MHz) δ 177.3, 145.8, 135.1, 133.8, 130.6, 126.1, 123.3, 74.1, 56.5, 54.1, 40.8, 33.1, 26.6, 23.5. MS (APCI) m/z = 323.1 ($M + 1$).

trans-3-[3-Chloro-4-(pyrrolidin-1-ylmethyl)phenyl]-N-methylcyclobutanecarboxamide (18). TFA (48 mL) was added to a solution of **16** (10.0 g, 31.4 mmol) in DCE (202 mL), and the resulting mixture was heated at 75 °C for 18 h and concentrated. The crude TFA salt of 3-[3-chloro-4-(pyrrolidin-1-ylmethyl)phenyl]-N-methylcyclobut-2-ene-1-carboxamide (**17**) thus obtained was redissolved in EtOH (130 mL) and hydrogenated (45 psi) at 60 °C in the presence of chlorotris(triphenylphosphine)rhodium(I) (Wilkinson's catalyst, 1.5 g). After 2 h, the mixture was cooled and concentrated. The residue was redissolved in 1 N aqueous HCl (100 mL) and washed twice with EtOAc (2×100 mL). The aqueous layer was then made basic with 1 N aqueous NaOH (100 mL) and extracted with EtOAc (2×500 mL). The combined organic phases were dried over MgSO_4 , filtered, and concentrated. Chromatography with a gradient of 5–15% MeOH in CH_2Cl_2 containing 0.25% NH_4OH gave a mixture of cis and trans isomers of the title compound (4.6 g, 48% yield). These isomers were separated by preparative chromatography on a Chiralcel OD (10 cm \times 50 cm) column using heptane/*i*-PrOH (90/10) to yield the pure trans (3.6 g) and cis (0.52 g) isomers. **trans-3-[3-Chloro-4-(pyrrolidin-1-ylmethyl)phenyl]-N-methylcyclobutanecarboxamide (18)**: ^1H NMR (CDCl_3 , 400 MHz) δ 7.39 (d, J = 7.8, 1H), 7.22 (d, J = 1.6, 1H), 7.09 (dd, J = 7.8, 1.2, 1H), 5.58 (br s, 1H), 3.69–3.77 (singlet at 3.72 (2H) overlapping multiplet (1H), 3H total), 2.94–3.00 (m, 1H), 2.86 (d, J = 5.1, 3H), 2.65–2.72 (m, 2H), 2.55–2.60 (m, 4H), 2.31–2.38 (m, 2H), 1.75–1.83 (m, 4H). ^{13}C NMR (CDCl_3 , 100 MHz) δ 175.8, 145.7, 134.4, 133.8, 130.6, 127.1, 124.7, 56.7, 54.2, 36.2, 36.1, 31.9, 26.4, 23.5. MS (APCI) m/z = 307.4 ($M + 1$).

1-{trans-3-[3-Chloro-4-(pyrrolidin-1-ylmethyl)phenyl]-cyclobutyl}-N-methylmethanamine (19). BH_3 –THF complex (1.0 M in THF, 319 mL, 319 mmol) was added to a solution of **18** (32.5 g, 106.2 mmol) in THF (516 mL), and the resulting solution was heated at 70 °C for 16 h. MeOH was added to quench the excess borane, and the heating was continued for another 16 h. The reaction mixture was cooled to room temperature and concentrated to yield a viscous oil which was redissolved in EtOAc (500 mL) and extracted into 6 N HCl (260 mL). The acidic aqueous phase was basified with 15% aqueous NaOH (500 mL) and extracted with EtOAc (2×750 mL). The extracts were dried over MgSO_4 , filtered, and concentrated to yield 30.3 g of crude product. Chromatography with a gradient of 5–100% MeOH in CH_2Cl_2 containing 0.25% NH_4OH afforded the title compound (23.7 g, 77% yield) as a colorless viscous oil. ^1H NMR (CDCl_3 , 400 MHz) δ 7.39 (d, J = 7.9, 1H), 7.23 (d, J = 1.7, 1H), 7.10 (dd, J = 7.9, 1.7, 1H), 3.73 (s, 2H), 3.55 (tt, J = 8.3, 8.2, 1H), 2.79 (d, J = 7.5, 2H), 2.56–2.61 (m, 4H), 2.48 (s, 3H) overlapping 2.44–2.51 (m, 1H), 2.21–2.31 (m, 2H), 2.12–2.18 (m, 2H), 1.76–1.83 (m, 4H). ^{13}C NMR (CDCl_3 , 100 MHz) δ 146.5, 134.1, 133.7, 130.5, 127.2, 124.7, 57.3, 56.7, 54.2, 36.6, 36.2, 32.4, 30.9, 23.5. MS (APCI) m/z = 293.2 ($M + 1$).

N-{[trans-3-[3-Chloro-4-(pyrrolidin-1-ylmethyl)phenyl]-cyclobutyl]methyl}-N-methylacetamide (4). Acetic anhydride (9.2 mL, 97 mmol) was added to a 0 °C solution of **19** (23.7 g, 81.2 mmol)

and Et₃N (22.6 mL, 162 mmol) in CH₂Cl₂ (230 mL). After the mixture was stirred for 30 min, 1 N aqueous NaOH (200 mL) was added and the phases were separated. The aqueous phase was extracted twice with EtOAc, and the combined organics were dried over MgSO₄, filtered, and concentrated to yield 29.2 g of crude product. Chromatography using a gradient of 5–20% MeOH in CH₂Cl₂ containing 0.1% NH₄OH yielded the title compound (27 g, 99%) as a colorless, viscous oil. This was dissolved in EtOAc (200 mL) and treated with 2 M HCl in Et₂O (81.2 mL) to afford the mono-HCl salt of the title compound as a white solid (30.6 g, 99%). ¹H NMR (MeOH-*d*₄, 400 MHz) δ 7.70–7.73 (m, 1H), 7.50 and 7.46 (2 d, *J* = 1.7, 1H total), 7.40 and 7.36 (2 dd, *J* = 7.9, 1.5, 1H total), 4.57 (s, 2H), 3.70–3.82 (m, 3H), 3.53–3.60 (m, 2H), 3.24 (m, 2H), 3.24 and 3.14 (2 s, 3H total), 2.72–2.86 (m, 1H), 2.17–2.38 (m, 9H), 2.02–2.12 (m, 2H). ¹³C NMR (MeOH-*d*₄, 100 MHz) δ 175.7, 175.4, 151.6, 151.5, 136.2, 134.3, 129.4, 129.3, 127.6, 127.5, 127.4, 127.3, 57.1, 55.9, 55.2, 54.7, 38.3, 37.2, 37.0, 36.0, 32.8, 32.6, 31.0, 30.4, 24.0, 20.2, 19.8. HRMS *m/z*, calcd (M + 1) 335.1884, observed 335.1880.

1-(4-Bromo-2-fluorobenzyl)pyrrolidine (20). 4-Bromo-2-fluorobenzyl bromide (375 g, 1.40 mol) was added in six portions to a 10 °C solution of pyrrolidine (363 g, 426 mL, 5.10 mol) in CH₃CN (2.75 L) while maintaining the temperature below 20 °C. After the mixture was stirred at room temperature for 4 h, the mixture was concentrated, water (500 mL) and saturated aqueous Na₂CO₃ (2 L) were added, and the mixture was extracted with CH₂Cl₂ (3 × 700 mL). The extracts were dried over Na₂SO₄, filtered, and concentrated, and the resulting light yellow oil was purified by vacuum distillation (\sim 1 mm, bp 125 °C) to yield the title compound (324.5 g, 90%) as a colorless oil. ¹H NMR (400 MHz, CDCl₃) δ 7.19–7.31 (m, 3H), 3.60 (d, *J* = 1.7, 2H), 2.48–2.52 (m, 4H), 1.74–1.77 (m, 4H). ¹³C NMR (CDCl₃, 100 MHz) δ 160.8 (d, *J*_{C–F} = 250), 132.3 (d, *J*_{C–F} = 6.0), 127.1 (d, *J*_{C–F} = 3.7), 125.3 (d, *J*_{C–F} = 14.7), 120.6 (d, *J*_{C–F} = 9.6), 118.7 (d, *J*_{C–F} = 25.7), 53.9, 52.2 (d, *J*_{C–F} = 1.5), 23.4. MS (APCI) *m/z* = 258.5 (M + 1).

***N*-Ethyl-3-[3-fluoro-4-(pyrrolidin-1-ylmethyl)phenyl]-3-hydroxy-*N*-methylcyclobutanecarboxamide (21).** This material was prepared as a waxy orange solid in 60% yield following the general procedure described for preparation of compound 16, by using 20 and substituting ethylmethylamine for methylamine. ¹H NMR (300 MHz, CDCl₃) δ 7.38 (t, *J* = 7.7, 1H), 7.18–7.25 (m, 2H), 5.10 and 4.84 (2 overlapping br s, 1H total), 3.68 (s, 2H), 3.48 and 3.33 (2 q, *J* = 7.2, 2H total), 3.13–3.23 (m, 1H), 3.00 and 2.97 (2 s, 3H total), 2.80–2.86 (m, 2H), 2.53–2.60 (m, 6H), 1.76–1.80 (m, 4H), 1.12–1.19 (m, 3H). ¹³C NMR (CDCl₃, 100 MHz) δ 175.9, 175.4, 162.3, 159.8, 146.9, 146.8, 131.3, 131.2, 124.6, 124.4, 120.4, 120.3, 112.3, 112.0, 73.9, 73.9, 73.7, 73.7, 53.9, 52.5, 52.4, 44.7, 43.0, 41.0, 40.8, 34.7, 33.5, 28.9, 28.3, 23.4, 14.0, 12.2. MS (APCI) *m/z* = 335.5 (M + 1).

***cis*-*N*-Ethyl-3-[3-fluoro-4-(pyrrolidin-1-ylmethyl)phenyl]-3-hydroxycyclobutanecarboxamide (23).** This material was prepared as a waxy orange solid in 49% yield from 20 following the general procedure described for compound 16 and substituting ethylamine for methylamine. ¹H NMR (400 MHz, CDCl₃) δ 7.36 (t, *J* = 7.9, 1H), 7.14–7.22 (m, 2H), 6.01 (br s, 1H), 5.77 (br s, 1H), 3.66 (d, *J* = 1.3, 2H), 3.28–3.35 (m, 2H), 2.71–2.82 (m, 3H), 2.47–2.55 (m, 6H), 1.74–1.79 (m, 4H), 1.15 (t, *J* = 7.3, 3H). ¹³C NMR (CDCl₃, 100 MHz) δ 176.5, 161.0 (d, *J*_{C–F} = 245.9), 146.8 (d, *J*_{C–F} = 7.4), 131.3 (d, *J*_{C–F} = 5.2), 124.1 (d, *J*_{C–F} = 15.5), 120.3 (d, *J*_{C–F} = 2.9), 112.0 (d, *J*_{C–F} = 22.8), 74.0 (d, *J*_{C–F} = 1.5), 53.8, 52.3 (d, *J*_{C–F} = 1.5), 40.9, 34.7, 33.2, 23.4, 14.7. MS (APCI) *m/z* = 321.3 (M + 1).

***cis*-3-[3-Fluoro-4-(pyrrolidin-1-ylmethyl)phenyl]-3-hydroxy-*N*-(2-methylpropyl)cyclobutanecarboxamide (24).** This material was prepared in 63% yield as a waxy orange solid from 20 following the general procedure described for compound 16 and substituting isobutylamine for methylamine. ¹H NMR (400 MHz, CDCl₃) δ 7.46

(t, *J* = 7.9, 1H), 7.18–7.24 (m, 2H), 6.10 (br s, 1H), 3.79 (s, 2H), 3.12 (t, *J* = 6.4, 2H), 2.77–2.83 (m, 3H), 2.62–2.70 (m, 4H), 2.45–2.55 (m, 2H), 1.75–1.86 (m, 4H), 0.87–0.99 [d at 0.92 (*J* = 6.6, 6H) overlapping m (1H)]. ¹³C NMR (CDCl₃, 100 MHz) δ 176.8, 161.0 (d, *J*_{C–F} = 245.9), 147.6 (d, *J*_{C–F} = 7.9), 131.7 (d, *J*_{C–F} = 4.4), 122.5 (d, *J*_{C–F} = 15.4), 120.6 (d, *J*_{C–F} = 4.7), 112.2 (d, *J*_{C–F} = 23.5), 74.1 (d, *J*_{C–F} = 1.5), 53.6, 51.9 (br s), 47.2, 41.0, 33.3, 28.5, 23.3, 20.0. MS (APCI) *m/z* = 349.4 (M + 1).

H₃ Receptor Binding Protocol. Cell paste was homogenized in 50 mM Tris-HCl buffer (pH 7.4 at 4 °C) containing 2.0 mM MgCl₂ using a Polytron at medium speed and spun in a centrifuge at 40000g for 10 min. The supernatant was discarded and the pellet suspended in 50 mM Tris-HCl buffer (pH 7.4 at 25 °C) containing 2 mM MgCl₂. Incubations were initiated by the addition of tissue homogenate to 96-well plates containing test drugs and radioligand (1.0 nM ³H-*N*- α -methylhistamine). Nonspecific binding was determined by radioligand binding in the presence of a saturating concentration of ciproxifan (10 μ M). After a 60 min incubation at room temperature, assay samples were rapidly filtered through Whatman GF/B filters that had been presoaked and dried in 0.5% polyethylenimine and rinsed with ice-cold 50 mM Tris-HCl buffer (pH 7.7 at 4 °C). Membrane-bound ³H-*N*- α -methylhistamine levels were determined by liquid scintillation counting of the filters in BetaScint on a Betaplate scintillation counter. The IC₅₀ (concentration at which 50% inhibition of specific binding occurs) was calculated by linear regression of the concentration–response data (logit transformation of the percent inhibition versus log of the concentration). *K_i* values were calculated based on the Cheng–Prusoff equation, *K_i* = IC₅₀/(1 + (*L*/*K_d*)), where *L* is the concentration of the radioligand used in the experiment and the *K_d* is the dissociation constant for the radioligand (determined previously by saturation analysis). Geometric mean values are expressed as p*K_i* \pm SEM.

H₃ cAMP Assay Protocol. *Cell Preparation.* HEK 293 cells stably expressing the human or rat histamine H₃ receptor and cAMP response element β -lactamase reporter gene were maintained in minimal essential media supplemented with 10% (v/v) fetal bovine serum, 2 mM glutamine, 0.1 mM nonessential amino acids, 1 mM sodium pyruvate, 25 mM HEPES, 300 μ g/mL Geneticin, and 50 μ g/mL Zeocin at 37 °C and 5% CO₂. Cells were harvested at 70–80% confluence and washed. A suspension of cells was added to each well of a 384-well, black clear-bottom poly-D-lysine coated plate such that each well received 25 000 cells (in 75 μ L). Plates were incubated at 37 °C/5% CO₂ overnight.

cAMP Assay. Following overnight incubation of the assay plate in a 37 °C/5% CO₂ incubator, 12.5 μ L of compound dilutions and maximum and minimum controls were added to the assay plate 10 min prior to addition of 12.5 μ L of forskolin or 12.5 μ L of forskolin/imetit. An amount of 25 μ L of phosphate-buffered saline was added to the blank wells. Plates were incubated for 4.5 h in a 37 °C/5% CO₂ incubator. Following the 4.5 h incubation, 50 μ L of MEM + 10 μ L of dye solution [loading dye solution was prepared at 6 \times final concentration: 6 μ L of solution A (1 mM CCF4-AM in dry dimethylsulfoxide) was added to 60 μ L of solution B (100 mg/mL Pluronic-F127 surfactant in dimethylsulfoxide and 0.1% acetic acid); the resulting solution was vortexed and added to 940 μ L of solution C (24% w/w PEG 400, 18% TR-40 by volume in water)] was added to each well and the assay plates were incubated for 90–120 min at room temperature and kept in the dark. The assay plates were then read using a Tecan SpectraFluor plate reader, with an excitation wavelength of 405 nm and emission wavelengths at 450 and 530 nm.

Data Analysis. Unconstrained sigmoidal curve fitting was used to estimate an IC₅₀ using GraphPad Prism. The *K_i* values were calculated from the IC₅₀ according to the Cheng–Prusoff equation *K_i* = (IC₅₀)/(1 + ([C]/EC₅₀)), where [C] is the concentration of the agonist (1 nM final imetit) used in the experiment and the EC₅₀ value is the EC₅₀ for the imetit determined in each experiment.

Phospholipidosis Assay Protocol. *Phospholipidosis Assay.* Transformed human liver epithelial cells (THLE) were purchased from American Type Culture Collection. Cells were kept in culture in bronchial epithelial growth media (Lonza) supplemented with 5 ng/mL human epidermal growth factor and 70 ng/mL phosphoethanolamine. All cell culture flasks and plates were precoated with bronchial epithelial basal medium supplemented with 0.01 mg/mL human fibronectin, 0.01 mg/mL BSA and 0.03 mg/mL collagen. Cells were maintained at 37 °C under 3.5% CO₂. Cells in logarithmic growth phase were seeded at a density of 1×10^4 per well in 96-well microplates. Test articles and the positive control, amiodarone (Sigma), were diluted in DMSO to 30 mM. Serial dilutions of all 30 mM stock concentrations were carried out in microplates, and 2 μ L of each concentration was transferred from the compound dilution plate to a new microplate. A fluorophore-labeled phospholipid, *N*-(7-nitrobenz-2-oxa-1,3-diazol-4-yl)-1,2-dihexadecanoyl-*sn*-glycero-3-phosphoethanolamine, triethylammonium salt (NBD-PE Invitrogen, CA, U.S.) was diluted with ethanol (1 mL) and sonicated for 10 min. The dye was then transferred into 250 mL of THLE medium and sonicated for an additional 30 min. The dye-supplemented medium was then filtered through a Millipore 22 μ m filter flask, and 200 μ L aliquots were added to each well of the intermediate plates containing 2 μ L of the test article and control dilutions to achieve final concentrations of 300, 100, 30, 10, 3, and 1 μ M test article or control.

At 24 hours after cell plating, the medium in each microplate was removed and compound dilutions in NBD-PE supplemented medium were added. Plates were returned to the incubator under the same conditions. At 24 hours after dosing, the medium was removed and cells were washed twice with 100 μ L of PBS. Following the wash, nucleic acid stain Hoechst 33342, diluted 1:1000 in PBS, was added and plates were incubated for 30 min at room temperature. Following incubation, cells were washed twice with 100 μ L of PBS. A final volume of 100 μ L of PBS was added, and plates were covered and left overnight at room temperature. The microplates were scanned in a Cellomics ArrayScan for quantitation of uptake of both Hoechst 33342, to identify cell nuclei, and NBD-PE, to determine phospholipid accumulation per cell. Compounds were classified as positive at the lowest dose for which the induction of phospholipid accumulation was 3-fold over background (Table 10).

Safety Studies. *In Vivo Tolerant Studies.* In vivo tolerant studies up to 2 weeks in duration were completed in Sprague–Dawley rats and beagle dogs. Drug formulations were prepared in 0.5% methylcellulose and administered at a dosage volume of 10 mL/kg in rats and 1 mL/kg in dogs. Monitored end points in these studies included clinical signs (daily), food intake (daily), body weight (daily), clinical pathology (hematology, serum chemistry, urinalysis; end of study), vital signs (heart rate, respiratory rate; dogs, predose and postdose at about T_{\max} at end of study), electrocardiogram (dogs, predose and postdose at about T_{\max} at end of study), plasma drug levels (day 1 and end of study; 4–5 time points on each sampling day), and gross/histopathology (end of dosing phase in repeat dose studies).

All procedures performed on these animals were in accordance with regulations and established guidelines and were reviewed and approved by an Institutional Animal Care and Use Committee or through an ethical review process. Convulsions in dogs were either self-limiting or required intervention with a standard anticonvulsant. Exposure and estimated safety margins derived from ETS in rats (14-day) and in dogs (single dose and 7-day) and are summarized in Table 11.

■ ASSOCIATED CONTENT

S Supporting Information. Cerep profile of lead compounds and spectral data for intermediates and final compounds. This material is available free of charge via the Internet at <http://pubs.acs.org>.

■ AUTHOR INFORMATION

Corresponding Author

*Phone: 860-715-4059. Fax: 860-686-6052. E-mail: travis.t.wager@pfizer.com.

Author Contributions

[†]T.T.W., B.A.P., and A.W.S. contributed to the writing of this manuscript.

■ ACKNOWLEDGMENT

The authors thank Joe Brady, Christopher O'Donnell, and Anabella Villalobos for helpful discussions; Ana Cobani, Elaine Greer, Stephen Anderson, and Margaret Landis for salt form and formulation evaluations; Daniel Virtue and Robert DePianta, Jr., Benjamin Hritzko, Chris Wood, Christopher Foti, Justin Ringling, Chris Caldwell, Marina Shalaeva, and Randy Smith for compound purifications, analytical assessments, and property measurements; James Candee and Jon Bordner for X-ray powder and single crystal crystallography support; Chester J. Siok, Darcy G. Izzarelli, Elizabeth E. Rubitski, David E. Johnson, Francis J. Sweeney, Holly D. Soares, Leslie K. Chambers, Bernard Fermini, Michelle A. Vanase-Frawley, Mihaly Hajos, Patricia A. Seymour, Weldon E. Horner, and William E. Hoffmann for providing in vitro selectivity and in vivo and biomarker data for the team; Bishop Wlodecki, Mark Elliot, Stanton McHardy, and Vinod Parikh for helpful discussions during the hunt for the best-in-class molecule; and Katherine Brighty for her insightful comments on this manuscript.

■ ABBREVIATIONS USED

ACh, acetylcholine; AD, Alzheimer's disease; ADHD, attention deficit hyperactivity disorder; ADME, absorption, distribution, metabolism, and excretion; cAMP, cyclic adenosine monophosphate; CMV, cardiomyocyte vacuoles; CNS, central nervous system; DA, dopamine; DCE, dichloroethane; DDI, drug–drug interactions; DMA, dimethylacetamide; DME, 1,2-dimethoxyethane; DMF, dimethylformamide; ER, efflux ratio; EtOAc, ethyl acetate; ETS, exploratory toxicology study; GPCR, G-protein-coupled receptor; HA, histamine; HBD, hydrogen bond donor; hERG, human ether-a-go-go-related gene; HLA, human lymphocyte assay; HLM, human liver microsome; HTS, high-throughput screening; IVMN, in vitro micronucleus; MDCK, Madin–Darby canine kidney; MDR, multidrug resistance; MED, minimally effective dose; MW, molecular weight; nAChR, nicotinic acetylcholine receptor; NaOH, sodium hydroxide; NE, norepinephrine; PCEC, projected clinically effective concentration; P-gp, P-glycoprotein; PK, pharmacokinetic; PL, phospholipidosis; RAMH, *R*- α -methylhistamine; RLM, rat liver microsome; rt, room temperature; SAR, structure–activity relationship; sc, subcutaneous; *t*-BuOK, potassium *tert*-butoxide; TEA, triethylamine; T3P, propylphosphonic anhydride; TEM, transmission electron microscope; TFA, trifluoroacetic acid; THF, tetrahydrofuran; THLE, transformed human liver epithelial; TI, therapeutic index; TPSA, topological polar surface area

■ REFERENCES

- (1) Ash, A. S. F.; Schild, H. O. Receptors mediating some actions of histamine. *Br. J. Pharmacol. Chemother.* **1966**, *27*, 427–439.
- (2) Black, J. W.; Duncan, W. A. M.; Durant, C. J.; Ganellin, C. R.; Parsons, E. M. Definition and antagonism of histamine H₂-receptors. *Nature* **1972**, *236*, 385–390.

- (3) Celanire, S.; Wijtman, M.; Talaga, P.; Leurs, R.; de Esch, I. J. P. Keynote review: histamine H₃ receptor antagonists reach out for the clinic. *Drug Discovery Today* **2005**, *10*, 1613–1627.
- (4) Łażewska, D.; Kieć-Kononowicz, K. Recent advances in histamine H₃ receptor antagonists/inverse agonists. *Expert Opin. Ther. Pat.* **2010**, *20*, 1147–1169.
- (5) Passani, M. B.; Lin, J.-S.; Hancock, A.; Crochet, S.; Blandina, P. The histamine H₃ receptor as a novel therapeutic target for cognitive and sleep disorders. *Trends Pharmacol. Sci.* **2004**, *25*, 618–625.
- (6) Barbier, A. J.; Bradbury, M. J. Histaminergic control of sleep–wake cycles: recent therapeutic advances for sleep and wake disorders. *CNS Neurol. Disord.: Drug Targets* **2007**, *6*, 31–43.
- (7) Levander, S.; Haegermark, O.; Staahle, M. Peripheral antihistamine and central sedative effects of three H₁-receptor antagonists. *Eur. J. Clin. Pharmacol.* **1985**, *28*, 523–529.
- (8) Arrang, J. M.; Garbarg, M.; Schwartz, J. C. Autoinhibition of brain histamine release mediated by a novel class (H₃) of histamine receptor. *Nature* **1983**, *302*, 832–837.
- (9) Brown, R. E.; Stevens, D. R.; Haas, H. L. The physiology of brain histamine. *Prog. Neurobiol. (Oxford, U. K.)* **2001**, *63*, 637–672.
- (10) Esbenshade, T. A.; Browman, K. E.; Bitner, R. S.; Strakhova, M.; Cowart, M. D.; Brioni, J. D. The histamine H₃ receptor: an attractive target for the treatment of cognitive disorders. *Br. J. Pharmacol.* **2008**, *154*, 1166–1181.
- (11) Tzavara, E. T.; Bymaster, F. P.; Overshiner, C. D.; Davis, R. J.; Perry, K. W.; Wolff, M.; McKinzie, D. L.; Witkin, J. M.; Nomikos, G. G. Procholinergic and memory enhancing properties of the selective norepinephrine uptake inhibitor atomoxetine. *Mol. Psychiatry* **2006**, *11*, 187–195.
- (12) Horner, W. E.; Johnson, D. E.; Schmidt, A. W.; Rollema, H. Methylphenidate and atomoxetine increase histamine release in rat prefrontal cortex. *Eur. J. Pharmacol.* **2007**, *558*, 96–97.
- (13) FDA. Atomoxetine (Marketed as Strattera) Information, 2005. <http://www.fda.gov/Drugs/DrugSafety/PostmarketDrugSafetyInformationforPatientsandProviders/ucm107912.htm>
- (14) Wernicke, J. F.; Kratochvil, C. J. Safety profile of atomoxetine in the treatment of children and adolescents with ADHD. *J. Clin. Psychiatry* **2002**, *63* (Suppl. 12), 50–55.
- (15) Fermini, B.; Fossa, A. A. The impact of drug-induced QT interval prolongation on drug discovery and development. *Nat. Rev. Drug Discovery* **2003**, *2*, 439–447.
- (16) Hosea, N. A.; Collard, W. T.; Cole, S.; Maurer, T. S.; Fang, R. X.; Jones, H.; Kakar, S. M.; Nakai, Y.; Smith, B. J.; Webster, R.; Beaumont, K. Prediction of human pharmacokinetics from preclinical information: comparative accuracy of quantitative prediction approaches. *J. Clin. Pharmacol.* **2009**, *49*, 513–533.
- (17) Gao, H.; Yao, L.; Mathieu, H. W.; Zhang, Y.; Maurer, T. S.; Troutman, M. D.; Scott, D. O.; Ruggeri, R. B.; Lin, J. In silico modeling of nonspecific binding to human liver microsomes. *Drug Metab. Dispos.* **2008**, *36*, 2130–2135.
- (18) Walker, J. Some new curarizing agents. *J. Chem. Soc.* **1950**, 193–197.
- (19) Sasaki, J. C.; Arey, J.; Eastmond, D. A.; Parks, K. K.; Grosovsky, A. J. Genotoxicity induced in human lymphoblasts by atmospheric reaction products of naphthalene and phenanthrene. *Mutat. Res., Genet. Toxicol. Environ. Mutagen.* **1997**, *393*, 23–35.
- (20) Smith, C. K.; Davies, G. J.; Dodson, E. J.; Moore, M. H. DNA–nogalamycin interactions: the crystal structure of d(TGATCA) complexed with nogalamycin. *Biochemistry* **1995**, *34*, 415–425.
- (21) Feigon, J.; Denny, W. A.; Leupin, W.; Kearns, D. R. Interactions of antitumor drugs with natural DNA: proton NMR study of binding mode and kinetics. *J. Med. Chem.* **1984**, *27*, 450–465.
- (22) Hancock, A. A.; Diehl, M. S.; Faghih, R.; Bush, E. N.; Krueger, K. M.; Krishna, G.; Miller, T. R.; Wilcox, D. M.; Nguyen, P.; Pratt, J. K.; Cowart, M. D.; Esbenshade, T. A.; Jacobson, P. B. In vitro optimization of structure activity relationships of analogues of A-331440 combining radioligand receptor binding assays and micronucleus assays of potential antiobesity histamine H₃ receptor antagonists. *Basic Clin. Pharmacol. Toxicol.* **2004**, *95*, 144–152.
- (23) Morini, G.; Comini, M.; Rivara, M.; Rivara, S.; Lorenzi, S.; Bordi, F.; Mor, M.; Flammini, L.; Bertoni, S.; Ballabeni, V.; Barocelli, E.; Plazzi, P. V. Dibasic non-imidazole histamine H₃ receptor antagonists with a rigid biphenyl scaffold. *Bioorg. Med. Chem. Lett.* **2006**, *16*, 4063–4067.
- (24) Clark, G. R.; Squire, C. J.; Gray, E. J.; Leupin, W.; Neidle, S. Designer DNA-binding drugs: the crystal structure of a meta-hydroxy analogue of Hoechst 33258 bound to d(CGCGAATTCGCG)₂. *Nucleic Acids Res.* **1996**, *24*, 4882–4889.
- (25) Miller, V. P.; Stresser, D. M.; Blanchard, A. P.; Turner, S.; Crespi, C. L. Fluorometric high-throughput screening for inhibitors of cytochrome P450. *Ann. N.Y. Acad. Sci.* **2000**, *919*, 26–32.
- (26) Aubrecht, J.; Osowski, J. J.; Persaud, P.; Cheung, J. R.; Ackerman, J.; Lopes, S. H.; Ku, W. W. Bioluminescent Salmonella reverse mutation assay: a screen for detecting mutagenicity with high throughput attributes. *Mutagenesis* **2007**, *22*, 335–342.
- (27) Homiski, M. L.; Muehlbauer, P. A.; Dobo, K. L.; Schuler, M. J.; Aubrecht, J. Concordance analysis of an in vitro micronucleus screening assay and the regulatory chromosome aberration assay using pharmaceutical drug candidates. *Environ. Mol. Mutagen.* **2010**, *51*, 39–47.
- (28) Feng, B.; Mills, J. B.; Davidson, R. E.; Mireles, R. J.; Janiszewski, J. S.; Troutman, M. D.; de Moraes, S. M. In vitro P-glycoprotein assays to predict the in vivo interactions of P-glycoprotein with drugs in the central nervous system. *Drug Metab. Dispos.* **2008**, *36*, 268–275.
- (29) Fox, G. B.; Pan, J. B.; Esbenshade, T. A.; Bitner, R. S.; Nikkel, A. L.; Miller, T.; Kang, C. H.; Bennani, Y. L.; Black, L. A.; Faghih, R.; Hancock, A. A.; Decker, M. W. Differential in vivo effects of H₃ receptor ligands in a new mouse dipsogenia model. *Pharmacol., Biochem. Behav.* **2002**, *72*, 741–750.
- (30) McLeod, R. L.; Rizzo, C. A.; West, R. E., Jr.; Aslanian, R.; McCormick, K.; Bryant, M.; Hsieh, Y.; Korfmacher, W.; Mingo, G. G.; Varty, L.; Williams, S. M.; Shih, N.-Y.; Egan, R. W.; Hey, J. A. Pharmacological characterization of the novel histamine H₃-receptor antagonist *N*-(3,5-dichlorophenyl)-*N'*-[[4-(1*H*-imidazol-4-ylmethyl)-phenyl]-methyl]-urea (SCH 79687). *J. Pharmacol. Exp. Ther.* **2003**, *305*, 1037–1044.
- (31) Smith, D. A.; van de Waterbeemd, H.; Walker, D. K. *Pharmacokinetics and Metabolism in Drug Design*, 2nd ed.; Wiley-VCH Verlag GmbH & Co. KGaA: New York, 2006; pp 19–37.
- (32) Price, D. A.; Blagg, J.; Jones, L.; Greene, N.; Wager, T. Physicochemical drug properties associated with in vivo toxicological outcomes: a review. *Expert Opin. Drug Metab. Toxicol.* **2009**, *5*, 921–931.
- (33) Hughes, J. D.; Blagg, J.; Price, D. A.; Bailey, S.; DeCrescenzo, G. A.; Devraj, R. V.; Ellsworth, E.; Fobian, Y. M.; Gibbs, M. E.; Gilles, R. W.; Greene, N.; Huang, E.; Krieger-Burke, T.; Loesel, J.; Wager, T.; Whiteley, L.; Zhang, Y. Physicochemical drug properties associated with in vivo toxicological outcomes. *Bioorg. Med. Chem. Lett.* **2008**, *18*, 4872–4875.
- (34) Wager, T. T.; Chandrasekaran, R. Y.; Hou, X.; Troutman, M. D.; Verhoest, P. R.; Villalobos, A.; Will, Y. Defining desirable central nervous system drug space through the alignment of molecular properties, in vitro ADME, and safety attributes. *ACS Chem. Neurosci.* **2010**, *1*, 420–434.
- (35) Wenlock, M. C.; Austin, R. P.; Barton, P.; Davis, A. M.; Leeson, P. D. A comparison of physicochemical property profiles of development and marketed oral drugs. *J. Med. Chem.* **2003**, *46*, 1250–1256.
- (36) Veber, D. F.; Johnson, S. R.; Cheng, H.-Y.; Smith, B. R.; Ward, K. W.; Kopple, K. D. Molecular properties that influence the oral bioavailability of drug candidates. *J. Med. Chem.* **2002**, *45*, 2615–2623.
- (37) Proudfoot, J. R. The evolution of synthetic oral drug properties. *Bioorg. Med. Chem. Lett.* **2005**, *15*, 1087–1090.
- (38) Pajouhesh, H.; Lenz, G. R. Medicinal chemical properties of successful central nervous system drugs. *NeuroRx* **2005**, *2*, 541–553.
- (39) Lipinski, C. A. Filtering in drug discovery. *Annu. Rep. Comput. Chem.* **2005**, *1*, 155–168.
- (40) Hitchcock, S. A.; Pennington, L. D. Structure–brain exposure relationships. *J. Med. Chem.* **2006**, *49*, 7559–7583.

- (41) Ploemen, J.-P. H. T. M.; Kelder, J.; Hafmans, T.; van de Sandt, H.; van Burgsteden, J. A.; Salemink, P. J. M.; van Esch, E. Use of physicochemical calculation of pKa and CLogP to predict phospholipidosis-inducing potential: a case study with structurally related piperazines. *Exp. Toxicol. Pathol.* **2004**, *55*, 347–355.
- (42) Morelli, J. K.; Buehrle, M.; Pognan, F.; Barone, L. R.; Fieles, W.; Ciaccio, P. J. Validation of an in vitro screen for phospholipidosis using a high-content biology platform. *Cell Biol. Toxicol.* **2006**, *22*, 15–27.
- (43) Hjelle, J. T.; Ruben, Z. Investigations in intracellular drug storage: localization of disbutamide in lysosomal and nonlysosomal vesicles. *Toxicol. Appl. Pharmacol.* **1989**, *101*, 70–82.
- (44) Rorig, K. J.; Ruben, Z.; Anderson, S. N. Structural determinants of cationic amphiphilic amines which induce clear cytoplasmic vacuoles in cultured cells. *Proc. Soc. Exp. Biol. Med.* **1987**, *184*, 165–171.
- (45) Ertl, P.; Rohde, B.; Selzer, P. Fast calculation of molecular polar surface area as a sum of fragment-based contributions and its application to the prediction of drug transport properties. *J. Med. Chem.* **2000**, *43*, 3714–3717.
- (46) Hanumegowda, U. M.; Wenke, G.; Regueiro-Ren, A.; Yordanova, R.; Corradi, J. P.; Adams, S. P. Phospholipidosis as a function of basicity, lipophilicity, and volume of distribution of compounds. *Chem. Res. Toxicol.* **2010**, *23*, 749–755.
- (47) Simplicio, A. L.; Clancy, J. M.; Gilmer, J. F. Prodrugs for amines. *Molecules* **2008**, *13*, 519–547.
- (48) Wager, T. T.; Hou, X.; Verhoest, P. R.; Villalobos, A. Moving beyond rules: the development of a central nervous system multi-parameter optimization (CNS MPO) approach to enable alignment of druglike properties. *ACS Chem. Neurosci.* **2010**, *1*, 435–449.
- (49) Stevens, C.; De Kimpe, N. A new entry into 2-azabicyclo-[2.1.1]hexanes via 3-(chloromethyl)cyclobutanone. *J. Org. Chem.* **1996**, *61*, 2174–2178.
- (50) Schultz, A. G.; McCloskey, P. J. Carboxamide and carbalkoxy group directed stereoselective iridium-catalyzed homogeneous olefin hydrogenations. *J. Org. Chem.* **1985**, *50*, 5905–5907.
- (51) Ertl, P. Polar surface area. *Methods Princ. Med. Chem.* **2008**, *37*, 111–126.
- (52) Wager, T. T.; Chandrasekaran, R. Y.; Butler, T. W. Preparation of Pyrrolidinylmethylphenylcyclobutanecarboxamides as Histamine H3 Receptor Antagonists. PCT Int. Appl. WO2007049123, 2007.